Editors' Suggestion

Revisiting flat band superconductivity: Dependence on minimal quantum metric and band touchings

Kukka-Emilia Huhtinen,[1,*] Jonah Herzog-Arbeitman,[2] Aaron Chew,[2] Bogdan A. Bernevig,[2,3,4] and Päivi Törmä[1,†]

[1]*Department of Applied Physics, Aalto University School of Science, FI-00076 Aalto, Finland*

[2]*Department of Physics, Princeton University, Princeton, New Jersey 08540, USA*

[3]*Donostia International Physics Center, P. Manuel de Lardizabal 4, 20018 Donostia-San Sebastian, Spain*

[4]*IKERBASQUE, Basque Foundation for Science, 48009 Bilbao, Spain*

(Received 21 March 2022; revised 18 June 2022; accepted 22 June 2022; published 26 July 2022)

A central result in superconductivity is that flat bands, though dispersionless, can still host a nonzero superfluid weight due to quantum geometry. We show that the derivation of the mean field superfluid weight in previous literature is incomplete, which can lead to severe quantitative and even qualitative errors. We derive the complete equations and demonstrate that the minimal quantum metric, the metric with minimum trace, is related to the superfluid weight in isolated flat bands. We complement this result with an exact calculation of the Cooper pair mass in attractive Hubbard models with the uniform pairing condition. When the orbitals are located at high-symmetry positions, the Cooper pair mass is exactly given by the quantum metric, which is guaranteed to be minimal. Moreover, we study the effect of closing the band gap between the flat and dispersive bands, and develop a mean field theory of pairing for different band-touching points via the S-matrix construction. In mean field theory, we show that a nonisolated flat band can actually be beneficial for superconductivity. This is a promising result in the search for high-temperature superconductivity as the material does not need to have flat bands that are isolated from other bands by the thermal energy. Our work resolves a fundamental caveat in understanding the relation of multiband superconductivity to quantum geometry, and the results on band touchings widen the class of systems advantageous for the search of high-temperature flat band superconductivity.

DOI: 10.1103/PhysRevB.106.014518

I. INTRODUCTION

Systems with dispersionless (flat) bands host exotic phenomena, as even small interactions will dominate the kinetic energy. For example, flat bands have been predicted to increase the critical temperature for superconductivity. Bardeen-Cooper-Schrieffer (BCS) theory predicts that the critical temperature is given by $T_c \propto \exp(-\frac{1}{|U|\rho_0(E_F)})$, where $|U|$ is the strength of the effective attractive interaction and $\rho_0(E_F)$ is the density of states at the Fermi surface. In a flat band, where the density of states diverges, T_c is proportional [1–3] to $|U|$, implying that the critical temperature can be much higher in flat bands than in dispersive bands at low interaction strengths.

However, the BCS critical temperature does not by itself indicate superconductivity, as it is only the critical temperature for Cooper pair formation. The Meissner effect and the possibility of dissipationless transport are also required. These are characterized by a nonzero superfluid weight D_s or, equivalently, superfluid stiffness [4]. Moreover, a nonzero D_s is a necessary condition for a nonzero Berezinsky-Kosterlitz-Thouless (BKT) transition temperature, which is the critical temperature for superconductivity in two dimensions. The superfluid weight is conventionally given by $D_s = n_e/m^*$, where n_e is the total particle density and m^* is the effective mass. In a flat band, single particles localize and m^* diverges, which indicates vanishing superfluid weight. However, in multiband models, the superfluid weight has an additional geometric contribution which can be nonzero even in the case of flat bands [5–8]. In the isolated band limit, this contribution has been shown [5] to be related to the quantum metric [9–11]. Monte Carlo results are in good agreement with this prediction [12–14]. Flat band superconductivity has attracted immense interest due to its relevance in magic-angle twisted bilayer graphene [15–17] and other moiré materials [18–22]. In particular, the potential importance of the geometric contribution to the superfluid weight has been shown in theoretical studies of twisted bilayer graphene [23–26], and has also been explored experimentally [27].

There is, however, a fundamental problem in the relation between the superfluid weight and the quantum metric as presented in previous literature. Consider a gedanken transformation that changes the orbital locations of a lattice model without altering the hopping terms. The superfluid weight is invariant under such transformations. On the other hand, the quantum metric depends not only on the tight-binding parameters of the lattice model, but also on the locations of the orbitals. We show that this discrepancy in mean field theory is resolved by properly accounting for the dependence of the order parameters on the magnetic vector potential. This dependence is crucial in multiband models, where the order parameters can have orbital-dependent phases. We show

*kukka-emilia.huhtinen@aalto.fi

†paivi.torma@aalto.fi

that accounting for the behavior of the order parameters is necessary even in systems with time-reversal symmetry and uniform pairing, contradicting previous literature [5,28]. We derive complete equations for the mean field superfluid weight, and show that the use of the simpler equations provided in previous literature can lead to quantitative and, in extreme cases, qualitative errors where the superfluid weight is incorrectly nonzero. We show that, in time-reversal-symmetric systems, the superfluid weight for isolated flat bands with uniform pairing is proportional to the *minimal* quantum metric, which is the quantum metric with the smallest possible trace.

These conclusions in mean field theory are mirrored by exact calculations of the Cooper pair mass in attractive Hubbard models possessing a uniform pairing condition. We find two contributions to the effective mass in perturbation theory: the quantum metric and a competing nonuniversal term. However, we show that the space-group symmetries strongly constrain the latter. If the orbitals are located at high-symmetry positions such that they are pinned in location by the lattice symmetries, this nonuniversal term vanishes and the quantum metric is the unique contribution to the Cooper pair mass. We propose a simple extension of the uniform pairing condition that guarantees the nonuniversal term vanishes.

In order to understand the behavior of nonisolated flat bands, we also study the effect of closing the gap between the flat band and dispersive bands. Remarkably, we show that a band touching can actually be beneficial for superconductivity (see Fig. 1). This is important, as it means that one does not need to find systems where the flat band is separated from the other bands by a large energy scale. If isolated bands were needed, trying to achieve a higher critical temperature would mean that larger band gaps were required to avoid thermal excitations to the other bands; this could be a severe limitation especially when searching for room-temperature superconductivity. Our results show that such isolation is not necessarily needed. In contrast, band touchings can enhance T_{BKT} or T_c.

We also investigate the effect of different types of band touchings, and show that the quantum geometry of the flat band alone is not sufficient to describe superconductivity in the nonisolated band limit: the type of band touching matters too, and can actually be used as a design degree of freedom when optimizing the critical temperature. We complement our numerical results with an analytic treatment of interacting bipartite crystalline lattices with mean field theory, yielding relations between the pairing strengths on different sublattices.

Overall, our results are promising for harnessing the potential of flat bands in increasing the critical temperature of superconductivity, illustrated by Fig. 1. For large interactions, dispersive band structures are often as good or better than flat band systems. In contrast, for weak interactions (typically $|U| < t$), flat bands provide a clear, even radical, advantage. This makes it possible to utilize a wider class of systems and materials for high-temperature superconductivity since interactions do not need to be strong. The potential of flat bands to offer high critical temperature even for weak interactions may also help avoid bipolarons and charge density waves competing with superconductivity at large interactions [29,30].

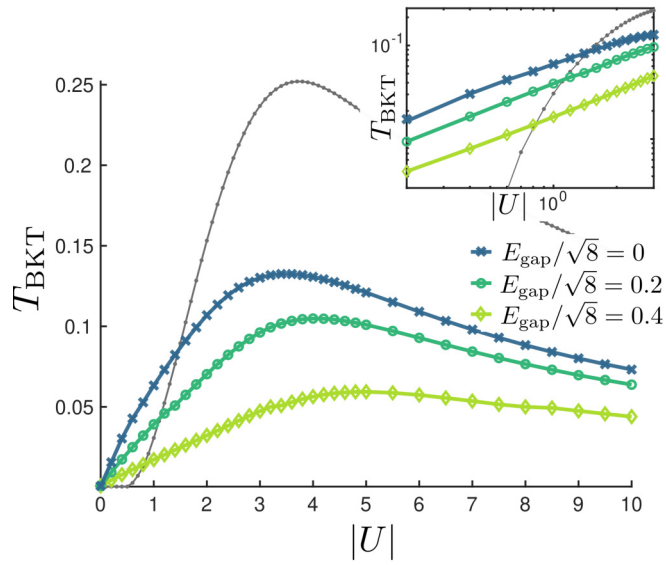

FIG. 1. BKT temperature computed for the square lattice (gray) and for the Lieb lattice with a half-filled flat band (blue, green, and yellow) with different values of the hopping staggering η (see Fig. 2). Inset: BKT temperature at interactions $0.2 \leqslant |U| \leqslant 3$. The flat band is isolated from the other bands by a band gap $E_{\mathrm{gap}} = \sqrt{8}\eta$. The highest BKT temperatures are obtained when $\eta = 0$, which corresponds to the situation where the gap between the flat band and dispersive bands closes, resulting in a linear band touching. The BKT temperature for the square lattice (gray) is exponentially suppressed at low interactions, whereas T_{BKT} on the isolated flat band is proportional to $|U|$. All energies are given in units of the average inter-lattice-site hopping energy t.

II. SUPERFLUID WEIGHT IN MULTIBAND MEAN FIELD MODELS

A. Model Hamiltonian

We study the Hubbard model on a multiband lattice

$$H = \sum_{\sigma} \sum_{i\alpha, j\beta} \left(t^{\sigma}_{i\alpha, j\beta} - \mu\delta_{i\alpha, j\beta}\right) c^{\dagger}_{i\alpha\sigma} c_{j\beta\sigma} + U \sum_{i\alpha} c^{\dagger}_{i\alpha\uparrow} c^{\dagger}_{i\alpha\downarrow} c_{i\alpha\downarrow} c_{i\alpha\uparrow}, \tag{1}$$

where i, j label the unit cells and α, β the orbitals in a unit cell. The hopping amplitude from site $j\beta$ to $i\alpha$ for spin σ is $t^{\sigma}_{i\alpha, j\beta}$ and $U < 0$ is the onsite interaction strength. The particle number is tuned by the chemical potential μ. We use the usual mean field approximation $U c^{\dagger}_{i\alpha\uparrow} c^{\dagger}_{i\alpha\downarrow} c_{i\alpha\downarrow} c_{i\alpha\uparrow} \approx \Delta_{i\alpha} c^{\dagger}_{i\alpha\uparrow} c^{\dagger}_{i\alpha\downarrow} + \mathrm{H.c.} - |\Delta_{i\alpha}|^2/U$, where $\Delta_{i\alpha} = U\langle c_{i\alpha\downarrow} c_{i\alpha\uparrow}\rangle$. We will focus on solutions where the order parameter is uniform on each orbital, $\Delta_{i\alpha} = \Delta_{\alpha}$, i.e., it does not depend on the unit-cell index i but can depend on the orbital index α.

B. Superfluid weight from the free energy

The superfluid weight can be defined as the change in free energy $F = \Omega + \mu N$, where Ω is the grand canonical potential and N is the particle number, due to a change in the phase of the order parameters $\Delta_{i\alpha} \to \Delta_{i\alpha} e^{2i\boldsymbol{q}\cdot\boldsymbol{r}_{i\alpha}}$ [5,31], with

$\boldsymbol{r}_{i\alpha}$ being the position of the site $i\alpha$:

$$[D_s]_{ij} = \frac{1}{V}\frac{d^2F}{dq_i dq_j}\bigg|_{\boldsymbol{q}=\boldsymbol{0}}. \tag{2}$$

Here, V is the volume of the system. The derivative is taken at a constant temperature, but the other thermodynamic variables are allowed to vary with $\boldsymbol{q}$.

Introducing the phase $e^{2i\boldsymbol{q}\cdot\boldsymbol{r}_{i\alpha}}$ into Eq. (1), the Fourier-transformed mean field Hamiltonian reads as

$$H(\boldsymbol{q}) = \sum_{\boldsymbol{k}} \boldsymbol{c}_{\boldsymbol{k}}^\dagger H_{\mathrm{BdG}}(\boldsymbol{k})\boldsymbol{c}_{\boldsymbol{k}} + \sum_{\boldsymbol{k}} \mathrm{Tr}H_{\boldsymbol{k}}^{\downarrow} - nN_c\mu - N_c\sum_{\alpha}\frac{|\Delta_\alpha(\boldsymbol{q})|^2}{U}, \tag{3}$$

$$H_{\mathrm{BdG}}(\boldsymbol{k}) = \begin{pmatrix} H_{\boldsymbol{q}+\boldsymbol{k}}^{\uparrow} - \mu\mathbf{1} & \boldsymbol{\Delta} \\ \boldsymbol{\Delta}^\dagger & -(H_{\boldsymbol{q}-\boldsymbol{k}}^{\downarrow})^* + \mu\mathbf{1} \end{pmatrix}, \tag{4}$$

where $\boldsymbol{c}_{\boldsymbol{k}} = (c_{\boldsymbol{q}+\boldsymbol{k},\alpha=1,\uparrow}, \ldots, c_{\boldsymbol{q}+\boldsymbol{k},\alpha=n,\uparrow}, c^\dagger_{\boldsymbol{q}-\boldsymbol{k},\alpha=1,\downarrow}, \ldots, c^\dagger_{\boldsymbol{q}-\boldsymbol{k},\alpha=n,\downarrow})^{\mathrm{T}}$ and n is the number of bands. The number of unit cells is denoted by N_c, and $\boldsymbol{\Delta} = \mathrm{diag}(\Delta_1, \ldots, \Delta_n)$. The matrix $H_{\boldsymbol{k}}^\sigma$ is the Fourier transformation of the kinetic Hamiltonian for spin σ, $[H_{\boldsymbol{k}}^\sigma]_{\alpha\beta} = \sum_i t^\sigma_{i\alpha,0\beta} e^{-i\boldsymbol{k}\cdot(\boldsymbol{R}_i+\boldsymbol{\delta}_\alpha-\boldsymbol{\delta}_\beta)}$, where $\boldsymbol{R}_i$ is the position of the ith unit cell and $\boldsymbol{\delta}_\alpha = \boldsymbol{r}_{i\alpha} - \boldsymbol{R}_i$. Here we have used the Fourier transformation

$$c_{\boldsymbol{k}\alpha\sigma} = \frac{1}{\sqrt{N_c}}\sum_i e^{-i\boldsymbol{k}\cdot(\boldsymbol{R}_i+\boldsymbol{\delta}_\alpha)} c_{i\alpha\sigma}, \tag{5}$$

which takes the intra-unit-cell positions of the orbitals into account. Another convention that is often used is

$$c_{\boldsymbol{k}\alpha\sigma} = \frac{1}{\sqrt{N_c}}\sum_i e^{-i\boldsymbol{k}\cdot\boldsymbol{R}_i} c_{i\alpha\sigma}, \tag{6}$$

which corresponds to setting all $\boldsymbol{\delta}_\alpha = \boldsymbol{0}$. This latter convention has the advantage of making the Hamiltonian explicitly periodic in reciprocal space. However, the choice of the orbital positions plays an essential role, as we will show, in relating the superfluid weight to quantum geometry.

The order parameters for a given chemical potential and temperature can be solved by minimizing the grand potential

$$\Omega = -\frac{1}{\beta}\sum_{\boldsymbol{k}}\sum_i \ln[1+\exp(-\beta E_{\boldsymbol{k},i})] + \sum_{\boldsymbol{k}} \mathrm{Tr}H_{\boldsymbol{k}}^{\downarrow} - nN_c\mu - N_c\sum_\alpha\frac{|\Delta_\alpha|^2}{U}, \tag{7}$$

where $E_{\boldsymbol{k},i}$ are the eigenvalues of the Bogoliubov–de Gennes Hamiltonian $H_{\mathrm{BdG}}(\boldsymbol{k})$. The particle number is controlled by the chemical potential μ, and fulfills the equation $N = -\partial\Omega/\partial\mu$.

Equation (2) can be cumbersome to use, as it requires knowledge of the state at nonzero $\boldsymbol{q}$. In previous literature [5], it has been shown that this equation simplifies to $[D_s]_{ij} = (1/V)\partial^2\Omega/\partial q_i\partial q_j|_{\boldsymbol{q}=\boldsymbol{0}}$ for systems with time-reversal symmetry (TRS), and assuming that the order parameter is always real, even for nonzero $\boldsymbol{q}$. The partial derivative is taken with all variables but $\boldsymbol{q}$ kept constant, meaning only knowledge of the state at $\boldsymbol{q} = \boldsymbol{0}$ is required. This simplified equation has been used, for example, to show that the superfluid weight of isolated flat bands is proportional to the quantum metric. A salient problem with that result, however, is that the quantum metric depends on the positions of the orbitals in a unit cell $\{\boldsymbol{\delta}_\alpha\}$ through Eq. (5). On the other hand, the superfluid weight is invariant under changes of $\{\boldsymbol{\delta}_\alpha\}$: this is immediately clear from the definition (2), given that the free energy does not depend on intra-unit-cell positions (when the hopping amplitudes $t_{i\alpha,j\beta}$ have been fixed constant). Using the terminology introduced in Ref. [32], the superfluid weight is geometry independent while the quantum metric is geometry dependent. The source of this discrepancy is the assumption that all order parameters are real even at nonzero $\boldsymbol{q}$. For a single-band model, this assumption can always be made because of the freedom in the phase of the order parameter. However, for a multiband model, the order parameters can have orbital-dependent phases and cannot, in general, be made simultaneously real by changing only the overall phase.

To understand how the problem arises, let us express $d^2F/dq_i dq_j$ in terms of partial derivatives of the grand canonical potential. For all the equations, we will fix the overall phase of the order parameters by imposing reality and positivity on a nonzero order parameter for one of the orbitals; we choose it to be $\Delta_1(\boldsymbol{q})$. For simplicity, we will focus here on a system with time-reversal symmetry, which implies that $\mu(\boldsymbol{q}) = \mu(-\boldsymbol{q})$ and $\Delta_\alpha(\boldsymbol{q}) = \Delta_\alpha^*(-\boldsymbol{q})$ [5]. Hence at $\boldsymbol{q} = \boldsymbol{0}$, the derivatives of the order parameters are purely imaginary and $d\mu/dq_i|_{\boldsymbol{q}=\boldsymbol{0}} = 0$. The general case without TRS is treated in Appendix A. Using the chain rule, the first derivative of the grand potential may be written as

$$\frac{d\Omega}{dq_i} = \frac{\partial\Omega}{\partial q_i} + \frac{\partial\Omega}{\partial\mu}\frac{d\mu}{dq_i} + \sum_\alpha \frac{\partial\Omega}{\partial\Delta_\alpha^I}\frac{d\Delta_\alpha^I}{dq_i} + \sum_\alpha \frac{\partial\Omega}{\partial\Delta_\alpha^R}\frac{d\Delta_\alpha^R}{dq_i}, \tag{8}$$

where we have used the notation $\Delta_\alpha^I = \mathrm{Im}(\Delta_\alpha)$ and $\Delta_\alpha^R = \mathrm{Re}(\Delta_\alpha)$. Taking the total derivative of Eq. (8) with reference to q_j and setting $\boldsymbol{q} = \boldsymbol{0}$ yields

$$\frac{d^2F}{dq_i dq_j}\bigg|_{\boldsymbol{q}=\boldsymbol{0}} = \frac{d^2\Omega}{dq_i dq_j}\bigg|_{\boldsymbol{q}=\boldsymbol{0}} - \frac{\partial\Omega}{\partial\mu}\frac{d^2\mu}{dq_i dq_j}\bigg|_{\boldsymbol{q}=\boldsymbol{0}} \tag{9}$$

$$= \frac{d}{dq_j}\frac{\partial\Omega}{\partial q_i}\bigg|_{\boldsymbol{q}=\boldsymbol{0}} \tag{10}$$

$$= \frac{\partial^2\Omega}{\partial q_i\partial q_j}\bigg|_{\boldsymbol{q}=\boldsymbol{0}} + \sum_\alpha \frac{\partial^2\Omega}{\partial\Delta_\alpha^I\partial q_i}\frac{d\Delta_\alpha^I}{dq_j}\bigg|_{\boldsymbol{q}=\boldsymbol{0}}. \tag{11}$$

We have used that $\partial\Omega/\partial\Delta_\alpha = 0$ at all $\boldsymbol{q}$, which is equivalent to the gap equation, and that the total particle number $N = -\partial\Omega/\partial\mu$ is constant. Due to TRS, the derivatives of the order parameters are purely imaginary at $\boldsymbol{q} = \boldsymbol{0}$ and $d\mu/dq_i|_{\boldsymbol{q}=\boldsymbol{0}} = 0$, which is why only the total derivatives of Δ_α^I appear on the third line. Since $\partial\Omega/\partial\Delta_\alpha = 0$ holds at all $\boldsymbol{q}$, we have

$$0 = \frac{d}{dq_i}\frac{\partial\Omega}{\partial\Delta_\alpha^I}\bigg|_{\boldsymbol{q}=\boldsymbol{0}} = \frac{\partial^2\Omega}{\partial q_i\partial\Delta_\alpha^I}\bigg|_{\boldsymbol{q}=\boldsymbol{0}} + \sum_\beta \frac{\partial^2\Omega}{\partial\Delta_\alpha^I\partial\Delta_\beta^I}\frac{d\Delta_\beta^I}{dq_i}\bigg|_{\boldsymbol{q}=\boldsymbol{0}}. \tag{12}$$

Using this identity, we can write Eq. (11) in a more concise form

$$\left.\frac{d^2F}{dq_i dq_j}\right|_{\boldsymbol{q}=\boldsymbol{0}} = \left.\frac{\partial^2\Omega}{\partial q_i \partial q_j}\right|_{\boldsymbol{q}=\boldsymbol{0}} - (d_i\Delta^I)^{\mathrm{T}}\partial^2_{\Delta^I}\Omega(d_j\Delta^I)|_{\boldsymbol{q}=\boldsymbol{0}}, \tag{13}$$

$$d_i\Delta^I = \left(\frac{d\Delta_2^I}{dq_i}, \ldots, \frac{d\Delta_n^I}{dq_i}\right)^{\mathrm{T}}, \tag{14}$$

$$\partial^2_{\Delta^I}\Omega = \begin{pmatrix} \frac{\partial^2\Omega}{\partial\Delta_2^I\partial\Delta_2^I} & \cdots & \frac{\partial^2\Omega}{\partial\Delta_2^I\partial\Delta_n^I} \\ \vdots & \ddots & \vdots \\ \frac{\partial^2\Omega}{\partial\Delta_n^I\partial\Delta_2^I} & \cdots & \frac{\partial^2\Omega}{\partial\Delta_n^I\partial\Delta_n^I} \end{pmatrix}. \tag{15}$$

The partial derivatives in $\partial^2_{\Delta^I}\Omega$ are taken by varying the involved order parameter while keeping all other variables constant.

Clearly, $d^2F/dq_i dq_j|_{\boldsymbol{q}=\boldsymbol{0}} = \partial^2\Omega/\partial q_i\partial q_j|_{\boldsymbol{q}=\boldsymbol{0}}$ when $d\Delta_\alpha^I/dq_i|_{\boldsymbol{q}=\boldsymbol{0}} = 0$. This holds if the order parameters are real also at nonzero $\boldsymbol{q}$. It has been argued in previous literature that the simplified equation $[D_s]_{ij} = (1/V)\partial^2\Omega/\partial q_i\partial q_j|_{\boldsymbol{q}=\boldsymbol{0}}$ can be used in systems with TRS, as the order parameters can be made real with a transformation $c_{i\alpha} \to c_{i\alpha}e^{i\theta_{i\alpha}(\boldsymbol{q})}$ [5]. This transformation has no effect on the free energy, and the superfluid weight remains unchanged. However, the terms on the right-hand side of Eq. (13) are *not* individually conserved under this transformation; they both change in such a way that the left-hand side of Eq. (13) remains invariant. Therefore, when using $[D_s]_{ij} = (1/V)\partial^2\Omega/\partial q_i\partial q_j|_{\boldsymbol{q}=\boldsymbol{0}}$, it is crucial to compute the partial derivative *after* the transformation $c_{i\alpha} \to c_{i\alpha}e^{i\theta_{i\alpha}(\boldsymbol{q})}$ is performed. In practice, one cannot assume that this simplified equation holds without knowledge of the behavior of the order parameters at nonzero $\boldsymbol{q}$, even in systems with TRS. This fact was correctly pointed out in Ref. [28]. However, it was stated therein that the additional terms are zero when the orbitals are equivalent. This is not generally the case: the introduction of the vector $\boldsymbol{q}$ in the system typically breaks the very symmetry which guaranteed equal pairing at the orbitals, meaning that the order parameters at $\boldsymbol{q} \neq \boldsymbol{0}$ can differ even if they are equal at $\boldsymbol{q} = \boldsymbol{0}$.

It is straightforward to show that the additional terms in Eq. (13) are always negative for $i = j$. The matrix $\partial^2_{\Delta^I}\Omega$ is the Hessian matrix of the grand canonical potential, and since the order parameters are a minimum of Ω, it is positive semidefinite. It follows immediately that $(d_i\Delta)^T\partial^2_{\Delta^I}\Omega(d_i\Delta) \geqslant 0$, which means that $(1/V)\partial^2\Omega/\partial q_i^2|_{\boldsymbol{q}=\boldsymbol{0}} \geqslant [D_s]_{ii}$. This implies that $\partial^2\Omega/\partial q_i\partial q_j$ can predict values that are much larger than the correct superfluid weight, including the case of indicating a nonzero superfluid weight when it is in fact vanishing.

The derivatives $d\Delta_\alpha/dq_i$ can be computationally expensive to evaluate, as they seem to require solving the gap equation at different nonzero $\boldsymbol{q}$. Remarkably, however, they can be determined with only knowledge of the ground state at $\boldsymbol{q} = \boldsymbol{0}$. This method relies on the system of equations given in Eq. (12), which can be written in matrix form as

$$(\partial^2_{\Delta^I}\Omega)d_i\Delta^I = -\boldsymbol{b_i}, \tag{16}$$

$$\boldsymbol{b_i} = \left(\frac{\partial^2\Omega}{\partial q_i\partial\Delta_2^I}, \ldots, \frac{\partial^2\Omega}{\partial q_i\partial\Delta_n^I}\right)^{\mathrm{T}}. \tag{17}$$

The derivatives of the order parameters are thus $d_i\Delta^I = -(\partial^2_{\Delta^I}\Omega)^{-1}\boldsymbol{b_i}$, which involves only partial derivatives of Ω and does not require knowledge of the state at nonzero $\boldsymbol{q}$.

C. Superfluid weight from linear response: Conventional and geometric contributions

In previous literature, the superfluid weight has been split into so-called conventional and geometric parts [5,6]. The conventional part is the only component present in single-band models, and is related to the derivatives of the band structure. It vanishes in the flat band limit. The geometric part is a purely multiband component which can be nonzero even on flat bands. Expressions for these components have been derived from linear response theory [6], but without accounting for the dependence of the order parameters on the vector potential. We compute the full mean field superfluid weight from linear response theory in Appendix D, and obtain

$$[D_s]_{ij} = \frac{1}{V}\sum_{\boldsymbol{k},ab}\frac{n_F(E_a)-n_F(E_b)}{E_b-E_a}[\langle\psi_a|\partial_i\widetilde{H}_{\boldsymbol{k}}|\psi_b\rangle\langle\psi_b|\partial_j\widetilde{H}_{\boldsymbol{k}}|\psi_a\rangle - \langle\psi_a|(\partial_i\widetilde{H}_{\boldsymbol{k}}\gamma^z + \delta_i\Delta)|\psi_b\rangle\langle\psi_b|(\partial_j\widetilde{H}_{\boldsymbol{k}}\gamma^z + \delta_j\Delta)|\psi_a\rangle] - \frac{1}{V_c}C_{ij}, \tag{18}$$

where

$$\partial_i\widetilde{H_{\boldsymbol{k}}} = \begin{pmatrix} \left.\frac{\partial H^{\uparrow}_{\boldsymbol{k}'}}{\partial k_i'}\right|_{\boldsymbol{k}'=\boldsymbol{k}} & 0 \\ 0 & \left.\frac{\partial(H^{\downarrow}_{\boldsymbol{k}'})^*}{\partial k_i'}\right|_{\boldsymbol{k}'=-\boldsymbol{k}} \end{pmatrix}, \quad \delta_i\Delta = \begin{pmatrix} 0 & \left.\frac{d\boldsymbol{\Delta}}{dq_i}\right|_{\boldsymbol{q}=\boldsymbol{0}} \\ \left.\frac{d\boldsymbol{\Delta}^{\dagger}}{dq_i}\right|_{\boldsymbol{q}=\boldsymbol{0}} & 0 \end{pmatrix}, \quad C_{ij} = \frac{1}{U}\sum_{\alpha}\left.\frac{d\Delta_\alpha}{dq_i}\frac{d\Delta_\alpha^*}{dq_j}\right|_{\boldsymbol{q}=\boldsymbol{0}} + \mathrm{H.c.} \tag{19}$$

Here, $\gamma^z = \sigma_z \otimes \mathbf{1}_{n\times n}$, where σ_i are Pauli matrices and $\mathbf{1}_{n\times n}$ is the $n \times n$ identity matrix. The eigenvalues and eigenvectors of H_{BdG} are E_a and $|\psi_a\rangle$, respectively, and $n_F(E)$ is the Fermi-Dirac distribution at E. The prefactor in (18) should be understood as $-\partial n_F(E)/\partial E$ when $E_a = E_b$. This expression differs from the one given in [6] by the addition of $\delta_i\Delta$ in the second term on the right-hand side of Eq. (18) and C_{ij}, which account for the derivatives of the order parameters.

To separate the conventional and geometric contributions of the superfluid weight, we write the eigenvectors of H_{BdG} in terms of the Bloch functions $|m_{\sigma,\boldsymbol{k}}\rangle$: $|\psi_a\rangle = \sum_{m=1}^{n}(w_{+,am}|+\rangle \otimes |m_{\uparrow,\boldsymbol{k}}\rangle + w_{-,am}|-\rangle \otimes |m^*_{\downarrow,-\boldsymbol{k}}\rangle)$,

where $|m_{\uparrow,\boldsymbol{k}}\rangle$ is the eigenvector of $H_{\boldsymbol{k}}^{\uparrow}$ with eigenvalue $\epsilon_{\uparrow,m,\boldsymbol{k}}$, $|m_{\downarrow,-\boldsymbol{k}}^{*}\rangle$ is the eigenvector of $(H_{-\boldsymbol{k}}^{\downarrow})^{*}$ with eigenvalue $\epsilon_{\downarrow,m,-\boldsymbol{k}}$, and $|\pm\rangle$ are the eigenvectors of σ_z with eigenvalues ± 1. Then, using the linear response result (18), we define

$$[D_{s,\mathrm{conv}}]_{\mu\nu} = \frac{1}{V}\sum_{\boldsymbol{k}}\sum_{mn} C_{nn}^{mm}[j_{\mu}^{\uparrow}(\boldsymbol{k})]_{mm}[j_{\nu}^{\downarrow}(-\boldsymbol{k})]_{nn}, \quad (20)$$

$$C_{pq}^{mn} = 4\sum_{ab}\frac{n_F(E_a)-n_F(E_b)}{E_b-E_a} w_{+,am}^{*} w_{+,bn} w_{-,bp}^{*} w_{-,aq}, \quad (21)$$

$$\begin{aligned}[j_{\mu}^{\sigma}(\boldsymbol{k})]_{mn} &= \langle m_{\sigma,\boldsymbol{k}}|\partial_{\mu}H_{\boldsymbol{k}}^{\sigma}|n_{\sigma,\boldsymbol{k}}\rangle \\ &= \delta_{mn}\partial_{\mu}\epsilon_{\sigma,m,\boldsymbol{k}} + (\epsilon_{\sigma,m,\boldsymbol{k}}-\epsilon_{\sigma,n,\boldsymbol{k}})\langle\partial_{\mu}m_{\sigma,\boldsymbol{k}}|n_{\sigma,\boldsymbol{k}}\rangle,\end{aligned} \quad (22)$$

where $\partial_{\mu} = \partial/\partial_{k_{\mu}}$. The geometric contribution is $D_{s,\mathrm{geom}} = D_s - D_{s,\mathrm{conv}}$.

The expression for the conventional contribution contains only single-band components of the current operators, $[j_{\mu}^{\sigma}(\boldsymbol{k})]_{mm} = \partial_{\mu}\epsilon_{\sigma,m,\boldsymbol{k}}$, and is the same as defined in previous literature [8]. The geometric contribution contains all other terms, including those arising from the derivatives of the imaginary components of the order parameters, which can only be nonzero in multiband models. This split into conventional and geometric contributions is independent of the choice of orbital positions, and as we show below, the geometric part is related to the minimal quantum metric in isolated flat bands. These definitions are valid in a system with TRS, where the derivatives of the order parameters can be made purely imaginary at $\boldsymbol{q} = 0$ [5]. In a system without TRS, there are additional terms arising from the derivatives of the real parts of the order parameters which can be nonzero even in a single-band system.

The superfluid weights derived from the free energy, Eq. (13), and by linear response, Eq. (18), are equal, as shown in Appendix E. We have verified numerically that both methods yield the same results in all examples studied in this paper.

III. QUANTUM METRIC AND ISOLATED FLAT BANDS

The quantum metric of a set of bands $\mathcal{S}$ is the real part of the quantum geometric tensor

$$\mathcal{B}_{ij}(\boldsymbol{k}) = 2\,\mathrm{Tr}\,P(\boldsymbol{k})\partial_i P(\boldsymbol{k})\partial_j P(\boldsymbol{k}), \quad (23)$$

where $P(\boldsymbol{k}) = \sum_{m\in\mathcal{S}}|m_{\boldsymbol{k}}\rangle\langle m_{\boldsymbol{k}}|$ is the projector into the Bloch states of the bands at $\boldsymbol{k}$. The quantum metric has been previously related to the superfluid weight, most prominently in the limit of isolated flat bands with TRS and where $\Delta_{\alpha} = \Delta$ for all orbitals where the flat band has a nonvanishing amplitude (this is the so-called uniform pairing condition) [5,6,33]. In such systems, the superfluid weight is given by

$$[D_s]_{ij} = \frac{4f(1-f)}{(2\pi)^{D-1}}|U|n_{\phi}\mathcal{M}_{ij}, \quad (24)$$

$$\mathcal{M}_{ij} = \frac{1}{2\pi}\int_{\mathrm{B.Z.}} d^D k\,\mathrm{Re}[\mathcal{B}_{ij}(\boldsymbol{k})]. \quad (25)$$

Here, f is the filling fraction of the band, $\mathcal{M}_{ij}$ is the quantum metric of the isolated flat band, n_{ϕ}^{-1} is the number of orbitals where the flat band states reside, and D is the dimension of the system. This result is derived from mean field theory using the equality $[D_s]_{ij} = (1/V)\partial^2\Omega/\partial q_i\partial q_j|_{\boldsymbol{q}=\boldsymbol{0}}$, or the equivalent linear response equations [5,6]. However, as we have shown in Sec. II, this equation is only accurate in special cases, even in systems with TRS and uniform pairing. We will show here that, nevertheless, it is actually possible to derive a general connection between the superfluid weight and the quantum geometry, but the relevant quantity turns out to be the *minimal* quantum metric, i.e., the quantum metric with the lowest possible trace over all possible orbital positions.

As stated in Sec. II B, in the presence of TRS,

$$\left.\frac{\partial^2\Omega}{\partial q_i^2}\right|_{\boldsymbol{q}=\boldsymbol{0}} \geqslant \left.\frac{d^2F}{dq_i^2}\right|_{\boldsymbol{q}=\boldsymbol{0}}. \quad (26)$$

Without TRS, this inequality may not be true when $d\mu/dq_i|_{\boldsymbol{q}=\boldsymbol{0}} \neq 0$ (see later in this section, Systems with broken time-reversal symmetry). When the inequality is saturated, the quantum metric is directly related to the superfluid weight. Otherwise, it gives an upper bound. We will first show that in systems with TRS, there always exists a point where the inequality is saturated. The property $\Delta(\boldsymbol{q}) = \Delta^{*}(-\boldsymbol{q})$ implies that

$$\left.\frac{d\Delta_{\alpha}}{dq_i}\right|_{\boldsymbol{q}=\boldsymbol{0}} = i\Delta_{\alpha}\left.\frac{d\theta_{\alpha}}{dq_i}\right|_{\boldsymbol{q}=\boldsymbol{0}}, \quad (27)$$

where θ_{α} is the phase of the order parameter $\Delta_{\alpha} = |\Delta_{\alpha}|e^{i\theta_{\alpha}}$. As before, we fix $\theta_1 = 0$, with Δ_1 a nonzero order parameter. It follows from Eq. (27) that $d\Delta_{\alpha}/dq_i = 0$ can only be nonzero if $d\theta_{\alpha}/dq_i = 0$ or if $\Delta_{\alpha} = 0$, meaning there is no pairing in the orbital.

Let us now assume that the order parameters for a choice of intra-unit-cell positions $\{\boldsymbol{\delta_{\alpha}}\}$ are $|\Delta_{\alpha}(\boldsymbol{q})|e^{i\theta_{\alpha}(\boldsymbol{q})}$. The order parameters in the same model for another choice of positions $\{\boldsymbol{\delta_{\alpha}}+\boldsymbol{x_{\alpha}}\}$ are $|\Delta_{\alpha}(\boldsymbol{q})|e^{i\widetilde{\theta}_{\alpha}(\boldsymbol{q})}$, with $\widetilde{\theta}_{\alpha}(\boldsymbol{q}) = \theta_{\alpha}(\boldsymbol{q}) - 2\boldsymbol{q}\cdot\boldsymbol{x}_{\alpha}$ (see Appendix B). Therefore,

$$\frac{d\widetilde{\theta}_{\alpha}(\boldsymbol{q})}{dq_i} = \frac{d\theta_{\alpha}(\boldsymbol{q})}{dq_i} - 2x_{\alpha}^{i}. \quad (28)$$

To set $d\Delta_{\alpha}/dq_i = 0$ and guarantee that $[D_s]_{ij} = (1/V)\partial^2\Omega/\partial q_i\partial q_j|_{\boldsymbol{q}=\boldsymbol{0}}$, we can thus shift the orbital positions by

$$x_{\alpha}^{i} = \frac{1}{2}\left.\frac{d\theta_{\alpha}(\boldsymbol{q})}{dq_i}\right|_{\boldsymbol{q}=\boldsymbol{0}}. \quad (29)$$

With the overall phase of the order parameters fixed, the order parameters are uniquely defined, and this shift is unique for all orbitals where $\Delta_{\alpha} \neq 0$. The resulting positions $\{\boldsymbol{\delta_{\alpha}}+\boldsymbol{x_{\alpha}}\}$ are independent of the particular initial choice of $\{\boldsymbol{\delta_{\alpha}}\}$ (see Appendix C). The quantum metric computed for this appropriate set of positions is related to the superfluid weight directly. We find precise analogs of these results in the uniform pairing Hubbard models considered in Sec. V.

We have shown that positions $\{\boldsymbol{\delta_{\alpha}}+\boldsymbol{x_{\alpha}}\}$ where D_s is related to the quantum metric exist, but using Eq. (29) to determine $\{\boldsymbol{x_{\alpha}}\}$ requires solving the gap equation. We will now show that it is possible to compute the correct quantum metric *without* solving the gap equation: it is the one with the smallest possible trace.

Since $\partial^2\Omega/\partial q_i\partial q_j \propto \mathcal{M}_{ij}$ and $\partial^2\Omega/\partial q_i^2 \geqslant d^2F/dq_i^2$, the result obtained from the quantum metric is always an

upper bound for the diagonal components of the superfluid weight. This upper bound is tight for the positions $\{\boldsymbol{\delta}_\alpha + \boldsymbol{x}_\alpha\}$, where it reaches a minimum. For an isolated flat band, the quantum metric with the *smallest possible integral of its diagonal components is thus proportional to the superfluid weight*. Since all diagonal components are minimized, this is the quantum metric with the smallest possible trace.

The relationship between the superfluid weight and the quantum metric has been used to derive lower bounds for the superfluid weight in flat band systems. Our result shows that for such a lower bound to be valid, it needs to be a lower bound for the quantum metric for any choice of the orbital positions. The validity of some lower bounds found in literature is discussed in Sec. VII.

A. Systems with broken time-reversal symmetry

Our result (13) is valid for time-reversal-symmetric systems. It can be straightforwardly generalized to be valid also for systems where TRS is broken (see Appendix A): $d^2F/dq_i dq_j$ will contain terms related to the derivatives of μ and the real parts of Δ_α. When $d\mu/dq_i|_{\boldsymbol{q}=\boldsymbol{0}} \neq 0$, the inequality (26) may not hold because the full Hessian matrix does not need to be positive semidefinite. When $d\mu/dq_i|_{\boldsymbol{q}=\boldsymbol{0}} = 0$, Eq. (26) holds. However, in contrast to systems with TRS, it may not be saturated for any choice of orbital positions: the derivatives of the *real parts* of the order parameters can be nonzero, and cannot be made zero by manipulating only the phases of the order parameters. Results relating the superfluid weight to the quantum metric can only be used in systems where $d|\Delta_\alpha|/dq_i|_{\boldsymbol{q}=\boldsymbol{0}} = 0$, provided the diagonal components $(1/V)\partial^2\Omega/\partial q_i^2|_{\boldsymbol{q}=\boldsymbol{0}}$ are minimized.

IV. EXAMPLE: SUPERFLUID WEIGHT, QUANTUM METRIC, AND ORBITAL POSITIONS IN THE LIEB LATTICE

To illustrate the importance of the additional terms in the superfluid weight derived in Sec. II, we study the superfluid weight in the Lieb lattice with staggered nearest-neighbor hopping amplitudes, shown in Fig. 2(a). The staggering is controlled by a parameter η so that the hopping amplitudes are $1+\eta$ within a unit cell and $1-\eta$ between unit cells. A nonzero η introduces a gap $E_{\text{gap}} = \sqrt{8}\eta$ between the flat band and dispersive bands [see Fig. 2(b)]. The parameter a controls the distance between the B site and the A/C sites in a unit cell. We use the average intersite hopping amplitude as our energy unit.

The complete equation (13) yields a result that is independent of the choice of orbital positions [see Figs. 2(c)–2(e)], contrary to $(1/V)\partial^2\Omega/\partial q_i \partial q_j|_{\boldsymbol{q}=\boldsymbol{0}}$. In the extreme case $\eta = 1$, when the lattice is disconnected and can clearly not support superconductivity, the correct superfluid weight is zero. However, using $\partial^2\Omega/\partial q_i \partial q_j|_{\boldsymbol{q}=\boldsymbol{0}}$ can in fact give a nonzero and quite large superfluid weight.

At $\eta = 0$, the simplified equation $[D_s]_{ij} = (1/V)\partial^2\Omega/\partial q_i \partial q_j|_{\boldsymbol{q}=\boldsymbol{0}}$ holds exactly when $a = \frac{1}{2}$, which corresponds to the Lieb lattice with C_{4v} symmetry when the convention given by Eq. (5) for the Fourier transformation

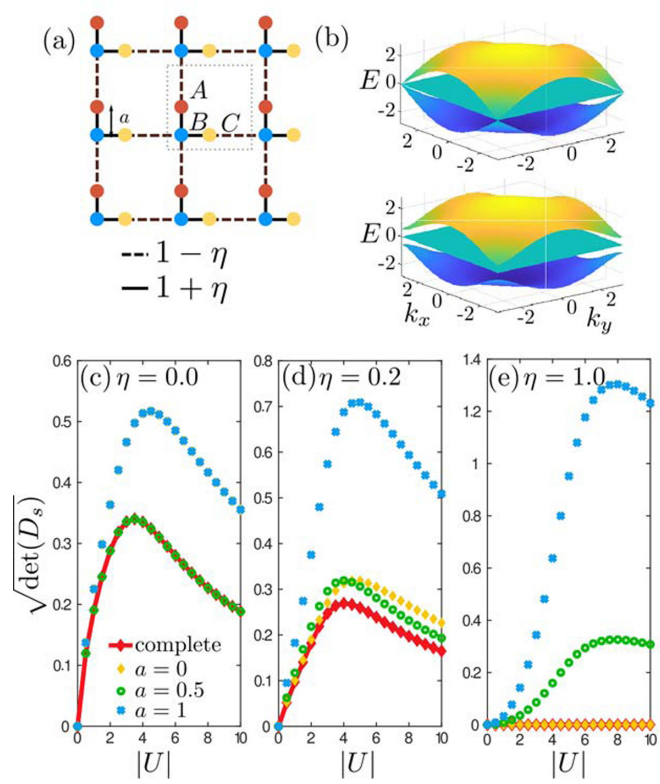

FIG. 2. (a) Lieb lattice with staggered hopping amplitudes. The position of the orbitals in the unit cell is controlled by the parameter a. We take the volume of the unit cell equal to 1. When $\eta = 0$ and $a = \frac{1}{2}$, the Lieb lattice possesses C_4 rotational symmetry, inversion symmetry, and reflection symmetry that interchanges the A, C orbitals, and thus belongs to symmetry group C_{4v}. Changing $\eta \neq 0$ or $a \neq \frac{1}{2}$ destroys the C_4 and inversion symmetries, thus reducing the symmetry group to C_s. Note that while only $\Delta_A = \Delta_C$, the flat band states have no weight in the B orbital, meaning the uniform pairing condition is fulfilled. (b) Single-particle band structure at $\eta = 0$ and 0.2. The flat band is separated from the other bands by a band gap $E_{\text{gap}} = \sqrt{8}\eta$. (c)–(e) Superfluid weight $\sqrt{\det(D_s)}$ in the Lieb lattice computed with (red, "complete") and without (the other colors) the corrections for three different choices of intra-unit-cell positions.

is used. This is explained by the equal hopping amplitudes in all directions: the systems with $a = \frac{1}{2} - x$ and $a = \frac{1}{2} + x$ are identical up to an overall rotation, and the additional terms are thus symmetric around $a = \frac{1}{2}$, where the minimum of $\partial^2\Omega/\partial q_i^2|_{\boldsymbol{q}=\boldsymbol{0}}$ occurs. Our proof in Sec. V generalizes this statement to all space groups. When η is increased and the C_4 symmetry is broken, the orbital positions for which $[D_s]_{ij} = (1/V)\partial^2\Omega/\partial q_i \partial q_j|_{\boldsymbol{q}=\boldsymbol{0}}$ shift continuously towards $a = 0$. Importantly, there is a wide parameter range where none of the choices $a = \frac{1}{2}$, 0, or 1 give the correct result when the derivatives of the order parameters are ignored. When $a = 0$ or 1, the position of the A, C orbitals is at the unit-cell origin (where the B orbitals are), and hence the Fourier transform (5) becomes identical to the other convention (6).

Finally, let us consider the role of the minimal quantum metric in our example case. In an earlier study [7], the quantum metric in the Lieb lattice has been related to the superfluid

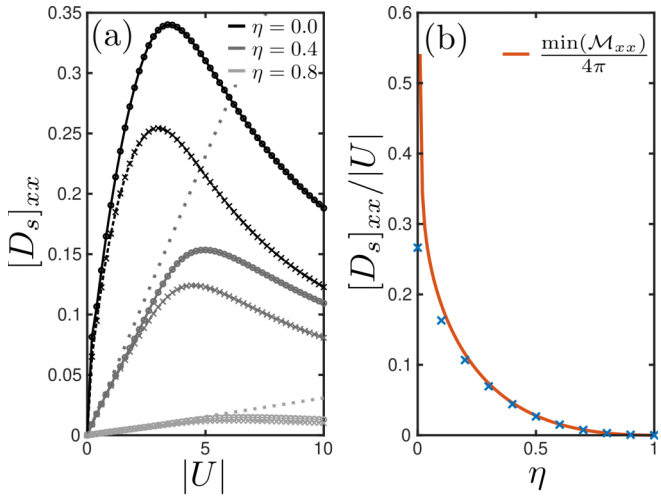

FIG. 3. (a) Superfluid weight (circles) and geometric contribution (crosses) as a function of $|U|$ at different η in the Lieb lattice. The dotted lines indicate the predictions from the minimal quantum metric. Only $[D_s]_{xx}$ is shown as the off-diagonal components of the superfluid weight tensor are very small for all parameters. At high interactions, the superfluid weight decays as $\propto 1/|U|$, which is a well-known behavior related to the formation of bound pairs in the BEC limit of the BCS-BEC crossover [34,35]. At low interactions, $D_s \propto |U|$ when the flat band is isolated. This linear behavior is visible in an increasingly wide range of interactions when η is increased. (b) $[D_s]_{xx}/|U|$ at low interactions obtained from a linear fit (crosses) and prediction for the slope from the minimal quantum metric.

weight. As shown in Fig. 3(a), the main contribution to the superfluid weight at low interactions is the geometric part, and the ratio D_{geom}/D_s approaches one in the isolated flat band limit. This is expected as the conventional contribution should vanish on a perfectly flat band. The prediction from the minimal quantum metric, shown in Fig. 3(b), is increasingly accurate with growing η.

V. COOPER PAIR MASS BEYOND MEAN FIELD

It has been shown that the two-body problem in a flat band gives for the bound pair a finite effective mass that is governed by quantum geometry [36,37]. For uniform pairing, the inverse effective mass can be approximately related to the quantum metric. Thus, pairs can move while single particles cannot, meaning that the qualitative picture given by mean-field superfluid weight calculations is already apparent at the two-body level. Here we calculate the Cooper pair mass in a full many-body treatment and without a mean field approximation. The mass is obtained from the spectrum of pair excitations of the ground state. It shows dependence on quantum geometry and allows relating the proper choice of quantum metric discussed above to the system symmetries.

We consider a family of positive-semidefinite, D-dimensional, attractive Hubbard models first introduced by Ref. [33] where the electron kinetic energy term has N_f perfectly flat zero-energy bands fulfilling a condition where the single-particle projectors $P(\boldsymbol{k})$ [see Eq. (23)] obey

$$\int \frac{d^D k}{(2\pi)^D} P_{\alpha\alpha}(\boldsymbol{k}) = n_\phi N_f \equiv \epsilon \tag{30}$$

for all orbitals $\alpha = 1, \ldots, n_\phi^{-1}$ where the pairing is nonzero. The condition (30) leads to the pairing gaps on different orbitals being the same, therefore, it is also referred to as the uniform pairing condition. We neglect the spin label, assuming that the model has time-reversal symmetry which relates the two projectors: $P_\uparrow(\boldsymbol{k}) = P_\downarrow^*(-\boldsymbol{k}) \equiv P(\boldsymbol{k})$. Upon projecting the many-body operators into the N_f flat bands, the kinetic energy vanishes and the Hamiltonian is given by the interaction term

$$H_U = -|U| \sum_{i\alpha} \bar{n}_{i\alpha,\uparrow} \bar{n}_{i\alpha,\downarrow} + \frac{n_\phi N_f}{2} |U| \bar{N}, \tag{31}$$

where $\bar{n}_{i,\alpha,\sigma}$ is the projected density operator in orbital α and spin σ, $\bar{N}$ is the projected total density operator. Reference [33] demonstrated that H_U possesses η-pairing ground states, that is, states with all particles paired. In forthcoming work [38], we show that the Cooper pair excitations on top of these ground states are exactly solvable thanks to the uniform pairing condition, and we are able to calculate their effective mass exactly.

The Cooper pair excitations are governed by the following single-particle Hamiltonian:

$$h_{\alpha\beta}(\boldsymbol{q}) = \int \frac{d^D k}{(2\pi)^D} P_{\alpha\beta}(\boldsymbol{q}+\boldsymbol{k}) P_{\beta\alpha}(\boldsymbol{k}). \tag{32}$$

We denote the eigenvalues of $h(\boldsymbol{q})$ as $\epsilon_\mu(\boldsymbol{q})$, where $\mu = 0, \ldots, n_\phi^{-1} - 1$. The many-body energy of the lowest-lying Cooper pair is $|U|(\epsilon - \epsilon_0(\boldsymbol{q}))$, where $\epsilon_0(\boldsymbol{q})$ is the *largest* eigenvalue of $h(\boldsymbol{q})$.

We now show that $\epsilon_\mu(\boldsymbol{q})$, and hence the Cooper pair spectrum, is invariant under a redefinition of the orbital locations $\boldsymbol{\delta}_\alpha \to \boldsymbol{\delta}_\alpha + \boldsymbol{x}_\alpha$ (leaving the hopping elements invariant). This must be the case physically because the choice of $\boldsymbol{x}_\alpha$ is just a convention for the Fourier transform. Since the redefinition means $P_{\alpha\beta}(\boldsymbol{k}) \to e^{-i\boldsymbol{k}\cdot(\boldsymbol{x}_\alpha - \boldsymbol{x}_\beta)} P_{\alpha\beta}(\boldsymbol{k})$, we see that $h_{\alpha\beta}(\boldsymbol{q})$ transforms under a redefinition of the orbitals as

$$\begin{aligned} h_{\alpha\beta}(\boldsymbol{q}) &\to e^{-i\boldsymbol{q}\cdot(\boldsymbol{x}_\alpha - \boldsymbol{x}_\beta)} \int \frac{d^D k}{(2\pi)^D} P_{\alpha\beta}(\boldsymbol{q}+\boldsymbol{k}) P_{\beta\alpha}(\boldsymbol{k}) \\ &= [V_{\boldsymbol{x}}^\dagger(\boldsymbol{q}) h(\boldsymbol{q}) V_{\boldsymbol{x}}(\boldsymbol{q})]_{\alpha\beta}, \end{aligned} \tag{33}$$

where we defined the diagonal unitary matrix $[V_{\boldsymbol{x}}(\boldsymbol{k})]_{\alpha\beta} = e^{i\boldsymbol{k}\cdot\boldsymbol{x}_\alpha}\delta_{\alpha\beta}$. We see explicitly that, although $h(\boldsymbol{q})$ is not invariant, its spectrum is.

The effective Cooper pair mass is given by

$$[m^{-1}]_{ij} = -|U| \frac{d^2 \epsilon_0(\boldsymbol{q})}{dq_i dq_j}\bigg|_{\boldsymbol{q}=\boldsymbol{0}} \tag{34}$$

which is computed from the spectrum of $h(\boldsymbol{q})$ and thus is manifestly invariant. Using perturbation theory, $\epsilon_0(\boldsymbol{q})$ can be easily calculated to second order in $\boldsymbol{q}$. At zeroth order $\epsilon_0(0) = \epsilon$, which corresponds to the constant eigenvector $u_0^\alpha = \sqrt{n_\phi}$. The first-order correction vanishes (showing the Cooper pair is stable), and we calculate two contributions at second order

in q_i:

$$\epsilon(\boldsymbol{q}) = \epsilon + \sum_{\mu=1}^{n-1} \frac{|u_\mu^\dagger(\boldsymbol{q}\cdot\nabla h)u_0|^2}{\epsilon-\epsilon_\mu(0)} + \frac{1}{2}q_iq_j\int\frac{d^Dk}{(2\pi)^D}\sum_{\alpha\beta}u_0^\alpha\partial_{ij}P_{\alpha\beta}(\boldsymbol{k})P_{\beta\alpha}(\boldsymbol{k})u_0^\beta, \quad (35)$$

noting that $\epsilon_\mu(0) < \epsilon$ are the eigenvalues of $h(0)$, so the first line is non-negative, and where ∇h is the gradient of h evaluated at $\boldsymbol{q} = 0$. After integration by parts, the integral in the second line yields

$$n_\phi\sum_{\alpha\beta}\int\frac{d^Dk}{(2\pi)^D}\partial_{ij}P_{\alpha\beta}P_{\beta\alpha} = -n_\phi\int\frac{d^Dk}{(2\pi)^D}\mathrm{Tr}\,\partial_iP\partial_jP = -\frac{n_\phi}{(2\pi)^{D-1}}\mathcal{M}_{ij}, \quad (36)$$

which is proportional to the quantum metric integrated over the Brillouin zone, i.e., $\mathcal{M}_{ij}$ defined in Eq. (24) (as $\mathrm{Tr}\,P\{\partial_iP,\partial_jP\} = \mathrm{Tr}\,\partial_iP\partial_jP$). Hence, Eq. (36) is negative semidefinite.

It is important to note that ∇h is not invariant under the choice of $\boldsymbol{x}_\alpha$, transforming as

$$\nabla h_{\alpha\beta} \to \nabla h_{\alpha\beta} - i(\boldsymbol{x}_\alpha - \boldsymbol{x}_\beta)h_{\alpha\beta}(0). \quad (37)$$

Nevertheless, it is possible to show that, up to a choice of origin, there is a unique choice of $\boldsymbol{x}_\alpha$ where $\nabla h u_0 = 0$ and the quantum metric is the sole contributor to the effective mass. Note that the $O(p^2)$ term in the first line of Eq. (35) competes with $-\mathcal{M}_{ij}$ in Eq. (36) because it is opposite in sign. Thus, the choice of $\boldsymbol{x}_\alpha$ where only the quantum metric is nonzero corresponds to the orbital positions of the minimal quantum metric.

A calculation using the uniform pairing condition results in an explicit form for the orbital shifts that make the quantum metric the sole contribution for the effective mass, namely,

$$[\epsilon - h(0)]\boldsymbol{x}_\alpha = -i[\nabla h u_0 n_\phi^{-1/2}]_\alpha. \quad (38)$$

This equation has a unique solution up to the overall choice of origin because $\epsilon - h(0)$ has a single zero eigenvalue corresponding to the uniform eigenvector u_0. With the orbital shifts $\boldsymbol{x}_\alpha$ given by Eq. (38), the effective mass becomes

$$[m^{-1}]_{ij} = \frac{n_\phi}{(2\pi)^{D-1}}|U|\mathcal{M}_{ij}. \quad (39)$$

Comparing this equation to Eq. (24), we find exact agreement with the mean field superfluid weight up to an overall factor of $4f(1-f)$, which is the Cooper pair density.

We now improve upon Eq. (39) in two ways. First we find that $\boldsymbol{x}_\alpha$ obey the space-group symmetries $g \in G$ of the Hamiltonian when the symmetric choice of Fourier convention [Eq. (5)] is used. In other words, when the symmetry-preserving positions of the orbitals are used, their deviations $\boldsymbol{x}_\alpha$ also obey the space-group symmetries. In many cases, this is tantamount to a proof that $\boldsymbol{x}_\alpha = 0$, meaning that the quantum metric is the *minimal* quantum metric, and is the Cooper pair mass. For instance, at $\eta = 0$ in the Lieb lattice with $a = \frac{1}{2}$, the A and C orbitals are related by C_4 symmetry and are invariant under C_2. There is no way to deform these orbitals off the positions $a = \frac{1}{2}$ without breaking C_2. Thus, $\boldsymbol{x}_\alpha = 0$, thereby explaining why $a = \frac{1}{2}$ is the correct choice to evaluate the minimal quantum metric in Fig. 2. By a similar argument, all orbitals at fixed high-symmetry positions necessarily have $\boldsymbol{x}_\alpha = \boldsymbol{0}$ because they are pinned by symmetries. In these cases, the minimal quantum metric is guaranteed to be the one computed using the physical positions in Eq. (5).

Second, we now propose a simple generalization of the uniform pairing condition that guarantees the quantum metric is minimal. We define the quantity

$$\varepsilon_\alpha(\boldsymbol{q}) = \int\frac{d^Dk}{(2\pi)^D}[P(\boldsymbol{k}+\boldsymbol{q})P(\boldsymbol{k})]_{\alpha\alpha} \quad (40)$$

which at $\boldsymbol{q} = 0$ yields $\varepsilon_\alpha = n_\phi N_f$, the uniform pairing condition in Eq. (30). It is then direct to check that

$$\varepsilon_\alpha(0) = n_\phi N_f \quad \text{(uniform pairing condition)},$$
$$\partial_i\varepsilon_\alpha(0) = 0 \quad \text{(minimal metric condition)}, \quad (41)$$

the latter condition being the many-body analog of Eq. (29), in that its solution sets the quantum metric to be minimal.

These results directly parallel those given by mean field theory in the above sections. We have shown that the Cooper pair effective mass is independent of the Fourier convention for the orbital positions. Furthermore, there exists a choice of orbital positions where the effective mass is determined by the quantum metric alone and at these positions the quantum metric is minimal. Under the uniform pairing condition, we provide an explicit formula for these positions in Eq. (38), to be compared to Eq. (29). The inclusion of crystalline symmetries constrains the positions: if the orbital positions are pinned by the symmetries, then the quantum metric evaluated for those positions must be minimal. Lastly, we established a generalization of the uniform pairing condition in Eq. (41) to determine when the quantum metric is minimal.

VI. NONISOLATED FLAT BANDS

The relationship of the minimal quantum metric and the superfluid weight indicates that the BKT transition temperature could be increased in systems with a high quantum metric. However, this is only valid in the isolated flat band limit. The quantum metric typically diverges when the band gap closes, but this is not an indication that the superfluid weight diverges. The superfluid weight is proportional to $|U|\mathcal{M}_{ij}$ only when the flat band is isolated, which requires that the interaction strength is small compared to the band gap (otherwise pairing would involve higher bands). Therefore, when the band gap shrinks, the largest $|U|$ for which the quantum metric is proportional to D_s decreases accordingly. The very large quantum metric that can be achieved with a small band gap is thus only relevant at very low interactions, where $[D_s]_{ij} \propto |U|\mathcal{M}_{ij}$ remains small. The divergence of the quantum metric is an indication that the contributions from the other bands are important at low $|U|$, and reduce the superfluid weight compared to the isolated flat band result. In the Lieb lattice, those contributions have been shown to curtail the divergence and lead to a finite superfluid weight [7]. An interesting question when searching for systems with high T_{BKT} is whether the critical temperature can still be large in the nonisolated band

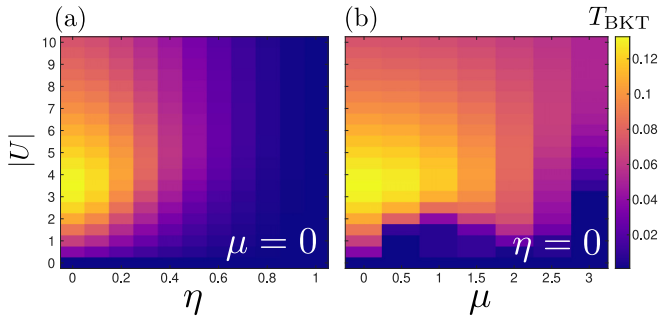

FIG. 4. BKT temperature in the Lieb lattice (a) as a function of the hopping staggering η and the interaction $|U|$, and (b) as a function of the chemical potential μ and the interaction. The largest BKT temperature occurs around interaction $U \approx -3.5$ with no hopping staggering, i.e., when the flat band is not isolated.

limit even though the contributions from dispersive bands are prominent. In repulsive models, a flat band near the Fermi surface has been predicted to be beneficial [39–42]. In attractive models, previous mean field studies have indicated that the superfluid weight has a nonlinear dependence on the interaction strength for nonisolated flat bands [7,34,43], but the additional terms we find in this work have not been taken into account. In this section, we show by continuously tuning the band gap that the superfluid weight and T_{BKT} can actually be maximal when there is a band touching. Furthermore, we study its dependence on different types of band touchings. We supplement our analysis of band-touching points by employing an S-matrix construction [44] to analyze bipartite lattices with band-touching points.

A. Effect of closing the band gap

As shown in Fig. 3, the superfluid weight in the Lieb lattice increases monotonically when η is decreased, and reaches its maximum when $\eta = 0$ for all interactions. For $\eta = 0$, when there is no band gap, the behavior is no longer exactly linear, which is consistent with previous literature such as [7], and [34,43] where it has been found that $D_s \propto |U|\ln(C/|U|)$, with C a constant.

The superfluid weight at zero temperature is an upper bound for the BKT temperature. However, it does not give the full picture: for instance, the zero-temperature superfluid weight in a dispersive band will typically be nonzero in the $U \to 0$ limit whereas it vanishes in a flat band. At $T = 0$, the superfluid weight will thus typically be smaller in a flat band than a dispersive band for small interactions, even though the BKT temperature is usually larger on the flat band (see Fig. 1). Here, we solve the BKT temperature from the universal relation [45–47]

$$T_{\mathrm{BKT}} = \frac{\pi}{8}\sqrt{\det[D_s(T_{\mathrm{BKT}})]}. \tag{42}$$

As is shown in Fig. 4(a), T_{BKT} mirrors the behavior of the superfluid weight and increases monotonically with η for all considered interactions. Moreover, the highest critical temperature as a function of μ is found for the half-filled flat band, showing that in this model, the highest possible critical temperature is achieved in the flat band when it is not isolated. Hence, the isolated flat band limit is not necessary to reach a high T_{BKT}, and a band touching could actually be beneficial for superconductivity. It is important to remember also that the flat band combined with a band touching yields a higher T_c than a usual dispersive band (e.g., square lattice) for small interactions $|U|$ (see Fig. 1).

B. Comparison of linear and quadratic band touchings

To study the effect of different types of band touchings on the superfluid weight, we use the method developed in Ref. [48] to construct flat band models where the dispersive bands can be modified by a parameter λ without affecting the Bloch functions of the flat band [see Fig. 5(a) and Appendix F]. We study two such models, constructed on a Lieb and kagome geometry. The Lieb model is constructed so that the band gap can be tuned with the staggering parameter η. Our energy unit is the average intersite hopping strength of the $\lambda = 0$ lattice model.

In the Lieb model, when η is nonzero, the superfluid weight at low interactions changes very little with λ [see Fig. 5(b)]. This is expected, as in the isolated band limit the superfluid weight is determined by quantum geometry, and the flat band has the same quantum metric for all λ. When the flat band is not isolated, differences in D_s occur already at vanishingly small interactions when varying λ [Fig. 5(c)]. Moreover, the ratio D_{geom}/D_s is much smaller for the quadratic than the linear band touching in both the Lieb [Fig. 5(d)] and kagome models [Fig. 5(g)]. The maximum of D_s is more pronounced in the linear model than the quadratic one in the models we studied, although the quadratic model has a higher D_s at low $|U|$ in the kagome model [Fig. 5(f)].

The geometry of the flat band therefore does not give the full picture in the nonisolated band limit: even though the Bloch functions of the flat band are left unchanged while the dispersive bands are modified, the superfluid weight differs. The behavior of the superfluid weight is thus dependent on the nature of the band touching.

C. Band-touching points from the S-matrix construction

The mean field behavior of the pairing gap in general lattices, with both isolated and nonisolated flat bands, can be understood using the S-matrix construction of Ref. [44]. This provides a description of the effect of band touchings on the pairing gap that is more general than given by the specific models considered above, and allows for an analytic solution in the mean field, yielding general results for quantities such as the pairing gap. The power of this approach is made evident as it yields self-consistent gap equations independent of the wave functions, allowing for an analysis of pairing strength as a function of the lattice parameters and dispersion.

The S-matrix construction employs a bipartite lattice with two unequal sublattices $L, \tilde{L}$, with the difference between the number of orbitals per unit cell $N_L - N_{\tilde{L}} = N_f$ being the number of flat bands. Band-touching points can be enforced in the model via irrep analysis of the symmetries [44]. The bipartite Hamiltonian in such models reads as

$$H_{\boldsymbol{k}} = \begin{bmatrix} 0 & S_{\boldsymbol{k}}^{\dagger} \\ S_{\boldsymbol{k}} & 0 \end{bmatrix}, \tag{43}$$

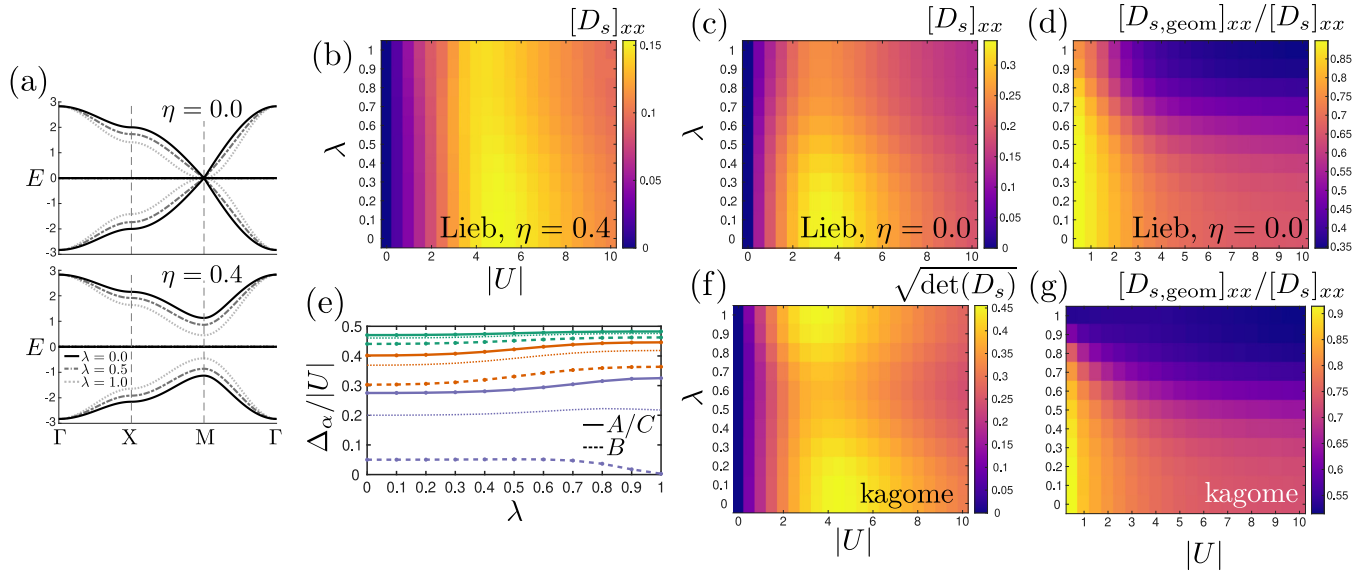

FIG. 5. (a) Band structure of the tunable Lieb model for different values of λ, at $\eta = 0$, i.e., in the presence of a band touching, and at $\eta = 0.4$. The band touching can be tuned from linear ($\lambda = 0$) to quadratic ($\lambda = 1$) at $\eta = 0$. At $\eta = 0.4$, the dispersive bands are modified without changing the quantum metric of the flat band. (b) Superfluid weight $[D_s]_{xx}$ for $\eta = 0.4$ in the Lieb model, when the flat band is separated from the other bands by a gap. At low $|U|$, D_s is independent of λ, but at intermediate $|U|$, the limit $\lambda = 0$, corresponding to a linear touching, has a more pronounced maximum. (c) Superfluid weight $[D_s]_{xx}$ and (d) ratio $[D_{s,\mathrm{geom}}]_{xx}/[D_s]_{xx}$ in the tunable Lieb lattice. The off-diagonal components of the superfluid weight are zero. The superfluid weight is largest in the linear model. (e) Order parameters Δ_α/U in the tunable Lieb lattice as a function of λ at interaction strengths $U = -1$ (blue), $U = -4$ (orange), and $U = -8$ (green). The order parameters in the A/C orbital (full line) are always equal, and are larger than the order parameter in the B orbital (dashed line). The dotted line shows the average of all order parameters. (f) $\sqrt{\det(D_s)}$ and (g) $[D_{s,\mathrm{geom}}]_{xx}/[D_s]_{xx}$ in the tunable kagome model. In this case, the off-diagonal components are not always zero. A similar behavior of the ratio $[D_{s,\mathrm{geom}}]_{ij}/[D_s]_{ij}$ is observed for all components. The maximum of $\sqrt{\det(D_s)}$ is slightly more pronounced in the linear model, but the superfluid weight at low $|U|$ is largest in the quadratic model.

where $S_{\boldsymbol{k}}^\dagger$ is an $N_{\tilde{L}} \times N_L$ rectangular matrix encoding the hopping between the two sublattices. These S-matrix Hamiltonians can be realized in actual physical materials [49]. The energies come in $\pm\epsilon_{\boldsymbol{k},m}$ pairs, where ϵ are the singular values of $S_{\boldsymbol{k}}$. Because $S_{\boldsymbol{k}}^\dagger$ maps C^{N_L} to $C^{N_{\tilde{L}}}$, there are at least $N_L - N_{\tilde{L}}$ vectors in the null space of $S_{\boldsymbol{k}}^\dagger$; these form the flat bands. One can introduce a quadratic Hamiltonian

$$H_{\mathrm{quad}} = H_{\boldsymbol{k}} \begin{bmatrix} I_{\tilde{L}\times\tilde{L}} & 0 \\ 0 & -I_{L\times L} \end{bmatrix} H_{\boldsymbol{k}} \tag{44}$$

which has eigenvalues $\pm\epsilon_{\boldsymbol{k},m}^2, 0$, and preserves the flat band wave functions. In the case of the Lieb lattice, this Hamiltonian is precisely the same as the Hamiltonian with quadratic band-touching points studied in Sec. VI B, obtained using the technique from Ref. [48] (see Appendix F for the tight-binding parameters of the model).

By adding attractive onsite interactions and assuming that the pairing is uniform within each sublattice, that is, there are two gaps Δ_L and $\Delta_{\tilde{L}}$ depending on the sublattice, we find the following self-consistent gap equations at $T = 0$ for $H_{\boldsymbol{k}}$:

$$N_L\Delta_L = \frac{|U|N_{\tilde{L}}}{2} f(\Delta) + \frac{|U|(N_L - N_{\tilde{L}})}{2}, \tag{45}$$

$$N_{\tilde{L}}\Delta_{\tilde{L}} = \frac{|U|N_{\tilde{L}}}{2} f(\Delta), \tag{46}$$

where $\Delta = \frac{1}{2}(\Delta_L + \Delta_{\tilde{L}})$ and

$$f(\Delta) = \frac{1}{N_{\tilde{L}}} \sum_{m=1}^{N_{\tilde{L}}} \int \frac{d^D k}{(2\pi)^D} \frac{\Delta}{\sqrt{\Delta^2 + \epsilon_{\boldsymbol{k},m}^2}}. \tag{47}$$

Here the sum is over the $N_{\tilde{L}}$ dispersive bands. The function f ranges from 0 for a perfectly flat band at zero kinetic energy to 1 for a gapped band at very large kinetic energy, and is a monotonically increasing function of Δ. Equation (46) always has a solution, and obeys the following properties:

$$N_L\Delta_L - N_{\tilde{L}}\Delta_{\tilde{L}} = \frac{|U|(N_L - N_{\tilde{L}})}{2}, \tag{48}$$

$$0 < \Delta_{\tilde{L}} < \Delta_L < \frac{|U|}{2}, \tag{49}$$

$$\frac{N_L - N_{\tilde{L}}}{4} < \frac{\Delta}{|U|} < \frac{1}{2}. \tag{50}$$

The first equality generalizes the result found in the Lieb lattice by Ref. [7], as it now applies to any bipartite lattice with uniform pairing within each sublattice, and agrees with our numerical calculations of the pairing gaps. The dispersion does not need to be gapless for this equality to hold; only the bipartite nature of the underlying lattice is required. These relations are proved in Appendix I. Regardless of the form of the bipartite lattice, even in the absence of a band touching, we find that the pairing strength on the larger sublattice Δ_L is always larger than the pairing on the smaller sublattice $\Delta_{\tilde{L}}$,

due to the fact that the flat bands greatly enhance the pairing for the sublattice L (see Appendix I), and both $\Delta_L, \Delta_{\tilde{L}}$ are bounded by quantities depending on the number of flat and dispersive bands.

Although the exact details of $f(\Delta)$ depend on the dispersion of the kinetic energy, the fact that it is bounded suggests that most of the gap strength comes from the flat band contribution which is universal. To maximize the strength of the pairing Δ_L, we note that the self-consistent equation for Δ_L depends only on the ratio of the number of bands of the sublattices $r = \frac{N_{\tilde{L}}}{N_L}$. This is saturated as $r \to 0$: thus, even in the presence of band-touching points, more flat bands per total bands enhance the superconducting gap at $T = 0$. If the dispersive bands are gapped from the flat bands, with the band gap $\gg |U|$, $f(\Delta) \to 0$. Thus, we approach the limit discussed in Ref. [5], where one may project the Hamiltonian into the flat bands and obtain an exactly solvable BCS ground state.

The quadratic band-touching point, i.e., the case of H_{quad}, has a different set of self-consistent gap equations (see Appendix I), due to the fact that the dispersive bands have different wave functions (though the flat band wave functions remain the same). The self-consistent equations still always possess a solution so long as flat bands exist. An analysis shows that the weighted difference reads as

$$N_L\Delta_L - N_{\tilde{L}}\Delta_{\tilde{L}} = \frac{|U|N_{\tilde{L}}}{2}[f(\Delta_L) - f(\Delta_{\tilde{L}})] + \frac{|U|(N_L - N_{\tilde{L}})}{2}, \tag{51}$$

which increases relative to Eq. (48) so long as $\Delta_L > \Delta_{\tilde{L}}$. We prove that there always exists a solution of the gap equations with this property (see Appendix I for more details).

In general, we expect the quadratic band touching will have a stronger pairing gap than the linear band touching: a higher density of states of the kinetic energy close to zero energy will raise Δ_L. This is what we observe in our numerical results for different band touchings in the Lieb lattice [Fig. 5(e)]. In contrast, the superfluid weight is larger for the linear model than the quadratic one. The pairing gap Δ_L is influenced by the density of states, which indeed is larger for a quadratic dispersion than a linear one, but the superfluid weight depends also on quantum geometry, which affects the ability of Cooper pairs to move. Thus, the two quantities can have qualitatively different behavior, contrary to what would be expected for an isolated flat band [5,6] where the superfluid weight is proportional to the pairing gap.

VII. REVISITING THE LITERATURE

The superfluid weight has been computed from mean field theory in a variety of multiband systems [6,7,13,14,28,34,43,50–53] including magic-angle twisted bilayer graphene [23–25]. The impact of the terms arising from the derivatives of the order parameters in Eq. (13) should be examined on a case-by-case basis. For example, the results for the Lieb lattice presented in [7] are close to the correct values for very small hopping staggering η while results for larger η are inaccurate. The results presented for the Mielke lattice with a flat band in [34] are accurate due to the spatial symmetries of the model.

In Ref. [28], the behavior of the order parameters was accurately taken into account when computing the superfluid weight, and the obtained mean field results agreed well with density matrix renormalization group (DMRG) calculations. In the sawtooth ladder, the mean field superfluid weight at low interactions was shown to agree very well with both DMRG and a flat-band projected analytical mean field computation of D_s, with all three methods predicting $\pi D_s \approx 0.40|U|$ for a half-filled flat band, and was noted to disagree with $\pi D_s = 0.6|U|$ obtained from the quantum metric. The estimate we find using the minimal quantum metric gives a slope of approximately $\pi D_s \approx 0.45|U|$, much closer to the correct result.

Expressions for the superfluid weight in terms of the quantum metric can be found in [6] for models without flat bands. For instance, in the isolated band limit,

$$[D_{s,\text{geom}}]_{ij} = \frac{2}{V}\Delta^2 \sum_{\boldsymbol{k}} \frac{\tanh(\beta E_{m,\boldsymbol{k}}/2)}{E_{m,\boldsymbol{k}}} \text{Re}(\mathcal{B}_{ij}), \tag{52}$$

where m labels the isolated band, which does not need to be flat. In this case, the minimal quantum metric is not always relevant, but one should instead minimize the above integral for $i = j$.

The relationship between the superfluid weight and quantum metric has been used to derive various bounds for the superfluid weight [5,6,13,23,54]. The lower bound given in [5] for time-reversal-symmetric systems in terms of the spin Chern number is valid, as it is a lower bound for the quantum metric regardless of the choice of orbital positions. On the other hand, bounds that depend on orbital positions, like the one proposed in [6] related to the integral of the absolute value of the Berry curvature, are only valid if they are a lower bound for all possible quantum metrics. The correct choice of orbital positions is thus needed to define an orbital-independent bound. This is also the case for the lower bound in terms of real-space invariants proposed in [13] for systems with obstructed Wannier orbitals or fragile topology. If the uniform pairing condition is satisfied, then space-group symmetries can guarantee that the minimal quantum metric is obtained for orbitals at the high-symmetry positions.

The two-body problem in a flat band was shown in Ref. [36] to give a finite effective mass for a pair, proportional to the "local" (spatially dependent) version of the quantum metric, which is independent of orbital positions. However, approximations were then used to connect the pair mass to the usual quantum metric. Our many-body Cooper pair calculation in Sec. V now shows that the correct choice is the minimal quantum metric.

Quantum geometry has been shown to be relevant also for Bose-Einstein condensation in flat bands [55,56]. The speed of sound and the excitation fraction were found to depend on generalized forms of the quantum metric, and the quantum distance between the flat band states, respectively. These quantities are invariant under the change of orbital positions. Under certain conditions, however, they were shown to reduce to the usual quantum metric and Hilbert-Smith quantum distance, and then (as well as in the superfluid density calculation

in [56]) one needs to pay attention to the choice of orbital positions.

Numerically exact methods such as quantum Monte Carlo do not require the same care as mean field theory with the behavior of the order parameters, as the interaction Hamiltonian of the exact Hubbard model does not depend on the vector field explicitly. Generally, it is important to make sure that all variables that may depend on the vector potential are properly taken into account.

In addition to the superfluid weight, the quantum metric has been related to the effective mass of two-body bounds states [36,37,57], conductivity [58], the orbital magnetic susceptibility [59,60], the velocity of the Goldstone mode [61], and other phenomena [62–68]. As shown here for the superfluid weight, whenever a connection is drawn between a physical quantity and the quantum metric, particular attention should be paid to the dependence of the quantum metric on the orbital positions.

VIII. CONCLUSIONS

We have derived complete equations for the mean field superfluid weight in multiband lattice models. These equations contain both the partial derivative of the grand potential, which gives a connection to quantum geometry, and terms that take into account the changes in the order parameter. The significance of the latter terms has been overlooked in the previous literature. We have shown that ignoring them can lead to quantitative as well as qualitative errors, where superconductivity can be predicted in systems where it is impossible. The use of the complete equations is thus crucial whenever studying multiband systems, such as moiré materials, as well as when searching for materials with particularly high critical temperatures.

Using our equations, we have shown that the superfluid weight in isolated flat bands is proportional to the *minimal* quantum metric, that is, the one with the smallest possible trace. A central discrepancy afflicting the current understanding of the connection between superconductivity and quantum geometry has been the following: the superfluid weight is manifestly independent on orbital positions, while the quantum metric, which has been shown to govern isolated flat band superconductivity, depends on them. Our finding that actually only the minimal quantum metric is relevant resolves this fundamental concern. Based on our results, bounds for the superfluid weight in terms of topological invariants in time-reversal-symmetric systems [5,23] are still valid, but other bounds which depend on the choice of orbital positions require more care.

The conclusions based on the mean field superfluid weight are corroborated by exact results derived for the Cooper pair mass. We generalized the uniform pairing condition in Eq. (41) to establish a minimal metric condition. When evaluated at the orbital positions satisfying the minimal metric condition, the Cooper pair mass is entirely determined by the quantum metric. Moreover, if the orbitals of the model are fixed by symmetries at high-symmetry points (maximal Wyckoff positions), then the minimal quantum metric is guaranteed to be obtained for these positions.

Importantly, our results show that in systems where TRS is broken, a relation between quantum geometry and superfluidity, and consequently topological bounds, does not exist in general. We identified sufficient conditions for having the connection to quantum geometry, namely, that the derivatives of the order parameter and chemical potential with respect to $\boldsymbol{q}$ have to vanish at $\boldsymbol{q} = \boldsymbol{0}$. Whether these conditions are also necessary remains a topic of future research, as well as the possible relations of the conditions to the crystalline symmetries, as in the time-reversal-symmetric, uniform pairing case.

Furthermore, we have shown that the quantum geometry of the flat band is not sufficient to describe the superfluid weight in the nonisolated band limit: its behavior depends not only on the flat band properties, but also on the nature of the band touching. Many flat band material candidates have band touchings [49]. Restricting to isolated flat bands would require materials and systems with a gap on the order tens of meV (the thermal energy). We have shown that this limitation is not necessary: in contrast, a band touching can enhance the critical temperature. This conclusion holds within the specific models considered by us, but is likely to be more general since the quantum metric of a flat band diverges when the gaps to the other bands are closed. This result is important for realizing the promise of high-temperature or even room-temperature superconductivity from flat bands. By results from S-matrix analysis, we developed universal relations relating the pairing gaps on bipartite lattices, and argued that the pairing gap is enhanced for quadratic over linear band touchings, a result opposite to what we saw numerically for the superfluid weight. This is understood as density of states determining the former while also quantum geometry is important for the latter. Our results inspire further engineering of band touchings to optimize the critical temperature of superconductivity, and determine the dominance of quantum geometry or the density of states.

ACKNOWLEDGMENTS

We thank A. Julku, L. Liang, S. Peotta, G. Salerno, and G. Topp for useful discussions. We acknowledge support by the Academy of Finland under Projects No. 303351 and No. 327293. K.-E.H. acknowledges support from the Magnus Ehrnrooth Foundation. B.A.B. and A.C. were supported by the ONR Grant No. N00014-20-1-2303, the Schmidt Fund for Innovative Research, Simons Investigator Grant No. 404513, the Gordon and Betty Moore Foundation through Grant No. GBMF8685 towards the Princeton theory program, and the Gordon and Betty Moore Foundation's EPiQS Initiative, Grant No. GBMF11070. Further support was provided by the NSF-MRSEC Grant No. DMR2011750, the BSF Israel US foundation Grant No. 2018226, and the Princeton Global Network Funds. B.A.B. acknowledges support from the Office of Naval Research Grant No. N00014-20-1-2303 and from the European Research Council (ERC) under the European Union's Horizon 2020 research and innovation programme (Grant Agreement No. 101020833). J.H.-A. is supported by a Marshall Scholarship funded by the Marshall Aid Commemoration Commission and a Hertz Fellowship. A.C. is supported by a Moore Postdoctoral Fellowship from the Gordon and Betty Moore Foundation.

APPENDIX A: GENERAL EQUATIONS FOR THE SUPERFLUID WEIGHT

In this Appendix, we derive the complete equations for the superfluid weight without assuming time-reversal symmetry. The system is invariant under a global change of phase of all order parameters, so we fix the overall phase by requiring that Δ_1 is real and positive, with Δ_1 a nonzero order parameter. We first apply the chain rule twice to the grand canonical potential to obtain

$$\begin{aligned}\frac{d^2\Omega}{dq_i dq_j} &= \frac{d}{dq_j}\frac{\partial\Omega}{\partial q_i} + \frac{d}{dq_j}\left(\frac{\partial\Omega}{\partial\mu}\right)\frac{d\mu}{dq_i} + \frac{\partial\Omega}{\partial\mu}\frac{d^2\mu}{dq_i dq_j} \\ &+ \sum_\alpha \frac{d}{dq_j}\left(\frac{\partial\Omega}{\partial\Delta_\alpha^R}\right)\frac{d\Delta_\alpha^R}{dq_i} + \sum_\alpha \frac{d}{dq_j}\left(\frac{\partial\Omega}{\partial\Delta_\alpha^I}\right)\frac{d\Delta_\alpha^I}{dq_i} \\ &+ \sum_\alpha \frac{\partial\Omega}{\partial\Delta_\alpha^R}\frac{d^2\Delta_\alpha^R}{dq_i dq_j} + \sum_\alpha \frac{\partial\Omega}{\partial\Delta_\alpha^I}\frac{d^2\Delta_\alpha^I}{dq_i dq_j}. \end{aligned} \tag{A1}$$

The particle number is fixed, meaning the second term on the right-hand side of the first line is zero. The third term is canceled by the derivative of μN when taking the derivative of the free energy $F = \Omega + \mu N$. Assuming that the order parameters solve the gap equation, $\partial\Omega/\partial\Delta_\alpha = 0$ for all $\boldsymbol{q}$, the terms on the second and third lines all vanish, and

$$\begin{aligned}\frac{d^2F}{dq_i dq_j} &= \frac{d}{dq_j}\frac{\partial\Omega}{\partial q_i} \\ &= \frac{\partial^2\Omega}{\partial q_i\partial q_j} + \frac{\partial^2\Omega}{\partial\mu\partial q_i}\frac{d\mu}{dq_j} \\ &+ \sum_\alpha\left(\frac{\partial^2\Omega}{\partial\Delta_\alpha^R\partial q_i}\frac{d\Delta_\alpha^R}{dq_j} + \frac{\partial^2\Omega}{\partial\Delta_\alpha^I\partial q_i}\frac{d\Delta_\alpha^I}{dq_j}\right)\Bigg|_{\boldsymbol{q}=\boldsymbol{0}}. \end{aligned} \tag{A2}$$

(A3)

This equation can be written in a more compact form by using that the particle number is kept fixed and $\partial\Omega/\partial\Delta_\alpha = 0$, implying that

$$\frac{d}{dq_i}\frac{\partial\Omega}{\partial\Delta_\alpha^R} = \frac{d}{dq_i}\frac{\partial\Omega}{\partial\Delta_\alpha^I} = \frac{d}{dq_i}\frac{\partial\Omega}{\partial\mu} = 0. \tag{A4}$$

This system of equations can be written in matrix form as $(\partial^2_{\Delta,\mu}\Omega)\boldsymbol{f_i} = -\boldsymbol{b_i}$, where

$$\partial^2_{\Delta,\mu}\Omega = \begin{pmatrix} \frac{\partial^2\Omega}{(\partial\Delta_1^R)^2} & \cdots & \frac{\partial^2\Omega}{\partial\Delta_1^R\partial\Delta_n^R} & \frac{\partial^2\Omega}{\partial\Delta_1^R\partial\Delta_2^I} & \cdots & \frac{\partial^2\Omega}{\partial\Delta_1^R\partial\Delta_n^I} & \frac{\partial^2\Omega}{\partial\Delta_1^R\partial\mu} \\ \vdots & \ddots & \vdots & \vdots & \ddots & \vdots & \vdots \\ \frac{\partial^2\Omega}{\partial\Delta_n^R\partial\Delta_1^R} & \cdots & \frac{\partial^2\Omega}{(\partial\Delta_n^R)^2} & \frac{\partial^2\Omega}{\partial\Delta_n^R\partial\Delta_2^I} & \cdots & \frac{\partial^2\Omega}{\partial\Delta_n^R\partial\Delta_n^I} & \frac{\partial^2\Omega}{\partial\Delta_n^R\partial\mu} \\ \frac{\partial^2\Omega}{\partial\Delta_2^I\partial\Delta_1^R} & \cdots & \frac{\partial^2\Omega}{\partial\Delta_2^I\partial\Delta_n^R} & \frac{\partial^2\Omega}{(\partial\Delta_2^I)^2} & \cdots & \frac{\partial^2\Omega}{\partial\Delta_2^I\partial\Delta_n^I} & \frac{\partial^2\Omega}{\partial\Delta_2^I\partial\mu} \\ \vdots & \ddots & \vdots & \vdots & \ddots & \vdots & \vdots \\ \frac{\partial^2\Omega}{\partial\Delta_n^I\partial\Delta_1^R} & \cdots & \frac{\partial^2\Omega}{\partial\Delta_n^I\partial\Delta_n^R} & \frac{\partial^2\Omega}{\partial\Delta_n^I\partial\Delta_2^I} & \cdots & \frac{\partial^2\Omega}{(\partial\Delta_n^I)^2} & \frac{\partial^2\Omega}{\partial\Delta_n^I\partial\mu} \\ \frac{\partial^2\Omega}{\partial\mu\partial\Delta_1^R} & \cdots & \frac{\partial^2\Omega}{\partial\mu\partial\Delta_n^R} & \frac{\partial^2\Omega}{\partial\mu\partial\Delta_2^I} & \cdots & \frac{\partial^2\Omega}{\partial\mu\partial\Delta_n^I} & \frac{\partial^2\Omega}{\partial\mu^2} \end{pmatrix}, \tag{A5}$$

$$\boldsymbol{f_i} = \left(\frac{d\Delta_1^R}{dq_i}, \ldots, \frac{d\Delta_n^R}{dq_i}, \frac{d\Delta_2^I}{dq_i}, \ldots, \frac{d\Delta_n^I}{dq_i}, \frac{d\mu}{dq_i}\right)^{\mathrm{T}}, \tag{A6}$$

$$\boldsymbol{b_i} = \left(\frac{\partial^2\Omega}{\partial q_i\partial\Delta_1^R}, \ldots, \frac{\partial^2\Omega}{\partial q_i\partial\Delta_n^R}, \frac{\partial^2\Omega}{\partial q_i\partial\Delta_2^I}, \ldots, \frac{\partial^2\Omega}{\partial q_i\partial\Delta_n^I}, \frac{\partial^2\Omega}{\partial q_i\partial\mu}\right)^{\mathrm{T}}. \tag{A7}$$

The order parameter Δ_1^I is absent as we have set the global phase of all order parameters by forcing Δ_1 real and positive. With these definitions, the total superfluid weight in Eq. (A3) can be written as

$$V[D_s]_{ij} = \frac{\partial^2\Omega}{\partial q_i\partial q_j}\bigg|_{\boldsymbol{q}=\boldsymbol{0}} - \boldsymbol{f_i}^{\mathrm{T}}(\partial^2_{\Delta,\mu}\Omega)\boldsymbol{f_j}\big|_{\boldsymbol{q}=\boldsymbol{0}}. \tag{A8}$$

The derivatives of the order parameters and chemical potential can be found by solving the state at nonzero $\boldsymbol{q}$ or from the system of equations $(\partial^2_{\Delta,\mu}\Omega)\boldsymbol{f_i} = -\boldsymbol{b_i}$ if the matrix $\partial^2_{\Delta,\mu}\Omega$ is invertible. If we had not fixed the overall phase of the order parameters, $\partial^2_{\Delta,\mu}\Omega$ would be singular. However, removing the line and column involving derivatives with reference to Δ_1^I from the Hessian matrix as we have done in the definition of $\partial^2_{\Delta,\mu}\Omega$ generally makes $\partial^2_{\Delta,\mu}\Omega$ nonsingular.

When the derivatives of the order parameters are purely imaginary, for example in systems with TRS, the additional terms $-\boldsymbol{f_i}^{\mathrm{T}}(\partial^2_{\Delta,\mu}\Omega)\boldsymbol{f_j}|_{\boldsymbol{q}=\boldsymbol{0}}$ appear only in multiband models. However, if the real part of the order parameters has a nonzero derivative, $[D_s]_{ij} = (1/V)\partial\Omega/\partial q_i\partial q_j|_{\boldsymbol{q}=\boldsymbol{0}}$ can be inaccurate even in single-band models, as the derivative cannot be made zero by changing the phase of the order parameter.

Here we have used only the order parameters as mean field parameters. If one included more parameters, for example Hartree terms, the $\boldsymbol{q}$ dependence of those parameters should be appropriately taken into account as well.

We note here that when $d\mu/dq_i|_{\boldsymbol{q}=\boldsymbol{0}} \neq 0$, the derivatives of the chemical potential may contribute to the superfluid weight. Both the definition $[D_s]_{ij} = (1/V)d^2\Omega/dq_i dq_j|_{\mu,\boldsymbol{q}=\boldsymbol{0}}$, where μ is fixed, and $[D_s]_{ij} = (1/V)d^2F/dq_i dq_j|_{N,\boldsymbol{q}=\boldsymbol{0}}$ used above have been used in literature, but it is unclear whether they always yield the same result at the mean field level. This ambiguity is related to the nonconservation of the particle number by the BCS Hamiltonian, which makes the introduction of the chemical potential more subtle at the mean field level than in the exact Hubbard Hamiltonian. If μ is thought

of as a Lagrange multiplier that should be solved to keep the average particle number constant, its dependence on $\boldsymbol{q}$ should be included.

APPENDIX B: IMPACT OF ORBITAL POSITIONS ON THE ORDER PARAMETERS

With our convention of Fourier transformation [Eq. (5)], the intra-unit-cell orbital positions $\boldsymbol{\delta_\alpha}$ appear in the Fourier-transformed kinetic Hamiltonians $[H_{\boldsymbol{k}}^\sigma]_{\alpha\beta} = -\sum_i t_{i\alpha,0\beta}^\sigma e^{-i\boldsymbol{k}\cdot(\boldsymbol{R}_i+\boldsymbol{\delta}_\alpha-\boldsymbol{\delta}_\beta)}$. Let us denote by $\widetilde{H}_{\boldsymbol{k}}^\sigma$ and $H_{\boldsymbol{k}}^\sigma$ the kinetic Hamiltonians with intra-unit-cell positions $\{\widetilde{\boldsymbol{\delta}_\alpha}\}$ and $\{\boldsymbol{\delta_\alpha}\}$, respectively. The two Hamiltonians are related by

$$\begin{aligned}[\widetilde{H}_{\boldsymbol{k}}^\sigma]_{\alpha\beta} &= -e^{-i\boldsymbol{k}\cdot(\widetilde{\boldsymbol{\delta}_\alpha}-\widetilde{\boldsymbol{\delta}_\beta})}\sum_i t_{i\alpha,0\beta}^\sigma e^{-i\boldsymbol{k}\cdot\boldsymbol{R}_i} \\ &= e^{-i\boldsymbol{k}\cdot(\widetilde{\boldsymbol{\delta}_\alpha}-\boldsymbol{\delta}_\alpha-\widetilde{\boldsymbol{\delta}_\beta}+\boldsymbol{\delta}_\beta)}[H_{\boldsymbol{k}}^\sigma]_{\alpha\beta}. \end{aligned} \tag{B1}$$

This can be rewritten in matrix form as $\widetilde{H}_{\boldsymbol{k}}^\sigma = V_{\boldsymbol{k}}^\dagger H_{\boldsymbol{k}}^\sigma V_{\boldsymbol{k}}$, where $V_{\boldsymbol{k}} = \mathrm{diag}(e^{i\boldsymbol{k}\cdot(\widetilde{\boldsymbol{\delta}_1}-\boldsymbol{\delta}_1)}, \ldots, e^{i\boldsymbol{k}\cdot(\widetilde{\boldsymbol{\delta}_n}-\boldsymbol{\delta}_n)})$.

To show how the orbital positions impact the order parameters, let us consider the corresponding Bogoliubov–de Gennes (BdG) Hamiltonians. By performing a unitary transformation $U\widetilde{H}_{\mathrm{BdG}}(\boldsymbol{k})U^\dagger$ with $U = \mathrm{diag}(V_{\boldsymbol{q}+\boldsymbol{k}}, V_{\boldsymbol{q}-\boldsymbol{k}}^\dagger)$, $\widetilde{H}_{\mathrm{BdG}}(\boldsymbol{k})$ becomes

$$U\widetilde{H}_{\mathrm{BdG}}(\boldsymbol{k})U^\dagger = \begin{pmatrix} H_{\boldsymbol{q}+\boldsymbol{k}}^\uparrow - \mu\mathbf{1} & V_{\boldsymbol{q}+\boldsymbol{k}}\boldsymbol{\Delta}V_{\boldsymbol{q}-\boldsymbol{k}} \\ V_{\boldsymbol{q}-\boldsymbol{k}}^\dagger\boldsymbol{\Delta}^\dagger V_{\boldsymbol{q}+\boldsymbol{k}}^\dagger & -\left(H_{\boldsymbol{q}-\boldsymbol{k}}^\downarrow\right)^* + \mu\mathbf{1} \end{pmatrix}. \tag{B2}$$

Assuming $\boldsymbol{\Delta}$ is diagonal, it commutes with V, and $V_{\boldsymbol{q}+\boldsymbol{k}}\boldsymbol{\Delta}V_{\boldsymbol{q}-\boldsymbol{k}} = \mathrm{diag}(\Delta_1 e^{2i\boldsymbol{q}\cdot(\widetilde{\boldsymbol{\delta}_1}-\boldsymbol{\delta}_1)}, \ldots, \Delta_n e^{2i\boldsymbol{q}\cdot(\widetilde{\boldsymbol{\delta}_n}-\boldsymbol{\delta}_n)})$. Thus, $\widetilde{H}_{\mathrm{BdG}}(\boldsymbol{k})$ with order parameters $(\Delta_1, \ldots, \Delta_n)$ has the same eigenvalues as $H_{\mathrm{BdG}}(\boldsymbol{k})$ with order parameters $(\Delta_1 e^{2i\boldsymbol{q}\cdot(\widetilde{\boldsymbol{\delta}_1}-\boldsymbol{\delta}_1)}, \ldots, \Delta_n e^{2i\boldsymbol{q}\cdot(\widetilde{\boldsymbol{\delta}_n}-\boldsymbol{\delta}_n)})$. Since the grand canonical potential depends only on the eigenvalues of the BdG Hamiltonian and the absolute value of the order parameters, the thermodynamic potentials are related by

$$\widetilde{\Omega}(\boldsymbol{q}, \mu, \Delta_\alpha) = \Omega(\boldsymbol{q}, \mu, \Delta_\alpha e^{2i\boldsymbol{q}\cdot(\widetilde{\boldsymbol{\delta}_\alpha}-\boldsymbol{\delta}_\alpha)}). \tag{B3}$$

The thermodynamic potential at the order parameters that solve the gap equation will always be the same for a given $\boldsymbol{q}$ and μ regardless of the intra-unit-cell positions. However, the order parameters that minimize the thermodynamic potential will have complex phases that depend on the intra-unit-cell positions. These phases can be sublattice dependent, and in the multiband case, they cannot in general be removed by a change in the overall phase of the order parameters.

APPENDIX C: POSITIONS FOR WHICH THE SUPERFLUID WEIGHT IS RELATED TO THE QUANTUM METRIC

The superfluid weight in a system with TRS is given by the simple equation $[D_s]_{ij} = (1/V)\partial^2\Omega/\partial q_i\partial q_j|_{\boldsymbol{q}=\boldsymbol{0}}$ when $-(d_i\Delta^I)^T\partial_{\Delta^I}^2\Omega(d_j\Delta^I)|_{\boldsymbol{q}=\boldsymbol{0}} = 0$ for all i, j. When $\partial_{\Delta^I}^2\Omega$ is invertible, this holds if and only if $d_i\Delta^I = 0$. This is the case when the overall phase of the order parameters is fixed.

The derivatives of the order parameters in a system with TRS are given by

$$\left.\frac{d\Delta_\alpha}{dq_i}\right|_{\boldsymbol{q}=\boldsymbol{0}} = i\left.\frac{d\Delta_\alpha^I}{dq_i}\right|_{\boldsymbol{q}=\boldsymbol{0}} = i\Delta_\alpha\left.\frac{d\theta_\alpha}{dq_i}\right|_{\boldsymbol{q}=\boldsymbol{0}}. \tag{C1}$$

As shown in Appendix B, if the solutions to the gap equation in a system with orbital positions $\{\boldsymbol{\delta_\alpha}\}$ are $\Delta_\alpha = |\Delta_\alpha|e^{i\theta_\alpha}$, the solutions with another choice of positions $\{\boldsymbol{\delta_\alpha}'\}$ are $\Delta_\alpha' = |\Delta_\alpha|e^{i\theta_\alpha'}$, where $\theta_\alpha' = \theta_\alpha - 2\boldsymbol{q}\cdot(\boldsymbol{\delta_\alpha}' - \boldsymbol{\delta_\alpha})$. The derivatives of the order parameters are thus related by

$$\left.\frac{d\Delta_\alpha^I}{dq_i}\right|_{\boldsymbol{q}=\boldsymbol{0}} = \Delta_\alpha\left.\frac{d\theta_\alpha}{dq_i}\right|_{\boldsymbol{q}=\boldsymbol{0}} = \Delta_\alpha\left.\frac{d\theta_\alpha'}{dq_i}\right|_{\boldsymbol{q}=\boldsymbol{0}} + 2\Delta_\alpha[\boldsymbol{\delta_\alpha}' - \boldsymbol{\delta_\alpha}]_i. \tag{C2}$$

The positions $\boldsymbol{\delta_\alpha}$ for which $d_i\Delta^I = 0$ can be solved directly from this equation once the derivative is known for some positions $\{\boldsymbol{\delta_\alpha^0}\}$. When $\partial_{\Delta^I}^2\Omega$ is invertible, the derivatives of the order parameters are uniquely defined, and the above equation gives a unique position $[\boldsymbol{\delta_\alpha}]_i = [\boldsymbol{\delta_\alpha^0}]_i + (d\theta_\alpha^0/dq_i)/2|_{\boldsymbol{q}=\boldsymbol{0}}$ for all sublattices where $\Delta_\alpha \neq 0$.

The initial choice of orbital positions $\{\boldsymbol{\delta}_\alpha^0\}$ is arbitrary, and we can verify that the solution $\{\boldsymbol{\delta_\alpha}\}$ where $d\Delta^I = 0$ remains the same with a different choice. If we pick another initial set of positions $\{\boldsymbol{\delta}_\alpha^1\}$, the positions for which $d\Delta_\alpha/dq_i|_{\boldsymbol{q}=\boldsymbol{0}} = 0$ are

$$\begin{aligned}[\boldsymbol{\delta_\alpha}]_i &= [\boldsymbol{\delta_\alpha^1}]_i + \frac{1}{2}\left.\frac{d\theta_\alpha^1}{dq_i}\right|_{\boldsymbol{q}=\boldsymbol{0}} = [\boldsymbol{\delta_\alpha^1}]_i - [\boldsymbol{\delta_\alpha^1} - \boldsymbol{\delta_\alpha^0}]_i + \frac{1}{2}\left.\frac{d\theta_\alpha^0}{dq_i}\right|_{\boldsymbol{q}=\boldsymbol{0}} \\ &= [\boldsymbol{\delta_\alpha^0}]_i + \frac{1}{2}\left.\frac{d\theta_\alpha^0}{dq_i}\right|_{\boldsymbol{q}=\boldsymbol{0}}, \end{aligned} \tag{C3}$$

for any sublattice α where $\Delta_\alpha \neq 0$. We used Eq. (C2) in the second equality. The positions $\{\boldsymbol{\delta_\alpha}\}$ are thus the same for any choice of initial orbital positions.

If we had not fixed the overall phase of the parameters at nonzero $\boldsymbol{q}$, the vector $d_i\Delta^I$ and the Hessian matrix $\partial_{\Delta^I}^2\Omega$ would read as

$$d_i\Delta^I = \left(\frac{d\Delta_1^I}{dq_i}, \ldots, \frac{d\Delta_n^I}{dq_i}\right)^{\mathrm{T}}, \tag{C4}$$

$$\partial_{\Delta^I}^2\Omega = \begin{pmatrix} \frac{\partial^2\Omega}{\partial\Delta_1^I\partial\Delta_1^I} & \cdots & \frac{\partial^2\Omega}{\partial\Delta_1^I\partial\Delta_n^I} \\ \vdots & \ddots & \vdots \\ \frac{\partial^2\Omega}{\partial\Delta_n^I\partial\Delta_1^I} & \cdots & \frac{\partial^2\Omega}{\partial\Delta_n^I\partial\Delta_n^I} \end{pmatrix}. \tag{C5}$$

These have the same form as in the main text, but with the addition of the terms related to Δ_1. The full Hessian matrix is not invertible, but has an eigenvector $\boldsymbol{v} = (\Delta_1, \ldots, \Delta_n)^T$ with a zero eigenvalue, which reflects the freedom in the phase of the order parameters [28]. In this case, $-(d_i\Delta^I)^T\partial_{\Delta^I}^2\Omega(d_j\Delta^I) = 0$ if and only if $d_i\Delta^I = C_i\boldsymbol{v}$, where C_i is a real number. Then from Eq. (C1), the positions for which $[D_s]_{ij} = (1/V)\partial^2\Omega/\partial q_i\partial q_j|_{\boldsymbol{q}=\boldsymbol{0}}$ are given by

$$[\boldsymbol{\delta_\alpha}]_i = [\boldsymbol{\delta_\alpha^0}]_i + \frac{1}{2}\left.\frac{d\theta_\alpha^0}{dq_i}\right|_{\boldsymbol{q}=\boldsymbol{0}} + C_i \tag{C6}$$

in sublattices where $\Delta_\alpha \neq 0$. Like before, $\{\boldsymbol{\delta_\alpha^0}\}$ are arbitrary orbital positions. If the overall phase of the order

parameters is not fixed, the positions for which $[D_s]_{ij} = (1/V)\partial^2\Omega/\partial q_i \partial q_j|_{\boldsymbol{q}=\boldsymbol{0}}$ are thus uniquely defined up to an overall translation by C_i.

APPENDIX D: SUPERFLUID WEIGHT FROM LINEAR RESPONSE THEORY

When computing the mean field superfluid weight from the current response as in [6], we get the same result as from $D_s = (1/V)\partial^2\Omega/\partial q_i \partial q_j|_{\boldsymbol{q}=\boldsymbol{0}}$. This is expected, as the dependence of the order parameters on the vector field is ignored. Here we compute the superfluid weight from linear response theory by taking this dependence into account, and obtain an expression that is equivalent with $[D_s]_{ij} = (1/V)d^2F/dq_i dq_j|_{\boldsymbol{q}=\boldsymbol{0}}$ when $d\mu/dq_i|_{\boldsymbol{q}=\boldsymbol{0}} = 0$.

Let us start from the mean field Hamiltonian

$$H_{\mathrm{MF}} = H_{\mathrm{kin}} + H_{\mathrm{int}}, \tag{D1}$$

$$H_{\mathrm{int}} = \sum_{i\alpha} \Delta_{i\alpha} c^\dagger_{i\alpha\uparrow} c^\dagger_{i\alpha\downarrow} + \Delta^*_{i\alpha} c_{i\alpha\downarrow} c_{i\alpha\uparrow} - \frac{|\Delta_{i\alpha}|^2}{U}, \tag{D2}$$

where $\Delta_{i\alpha} = U\langle c_{i\alpha\downarrow} c_{i\alpha\uparrow}\rangle$. The vector field is introduced using the standard Peierls substitution in the kinetic term, so that $t^\sigma_{i\alpha,j\beta}$ is rewritten as $t^\sigma_{i\alpha,j\beta}(\boldsymbol{A}) = t^\sigma_{i\alpha,j\beta}\exp(-i\int_{\boldsymbol{r}_{i\alpha}}^{\boldsymbol{r}_{j\beta}} \boldsymbol{A}\cdot d\boldsymbol{r})$. We assume that $\boldsymbol{A}$ varies slowly in space and time. Then, the hopping terms can be approximated by $t^\sigma_{i\alpha,j\beta}(\boldsymbol{A}) = t^\sigma_{i\alpha,j\beta} e^{-i\boldsymbol{A}(\boldsymbol{r}^{\mathrm{CM}}_{i\alpha,j\beta},t)\cdot\boldsymbol{r}^{\mathrm{rel}}_{i\alpha,j\beta}}$, where $\boldsymbol{r}^{\mathrm{rel}}_{i\alpha,j\beta} = \boldsymbol{r}_{i\alpha} - \boldsymbol{r}_{j\beta}$ and $r^{\mathrm{CM}}_{i\alpha,j\beta} = (\boldsymbol{r}_{i\alpha} + \boldsymbol{r}_{j\beta})/2$. The total current density induced by $\boldsymbol{A}$ is $j_\mu(\boldsymbol{r},t) = -\delta H(\boldsymbol{A})/\delta A_\mu(\boldsymbol{r},t)$, where $\delta/\delta A_\mu$ is the functional derivative with reference to A_μ.

We first expand the kinetic term up to second order in $\boldsymbol{A}$ around $\boldsymbol{A} = \boldsymbol{0}$ to obtain the functional derivative up to first order:

$$\frac{\delta H_{\mathrm{kin}}(\boldsymbol{A})}{\delta A_\mu(\boldsymbol{r},t)} = \sum_{\substack{i\alpha,j\beta \\ \boldsymbol{r}^{\mathrm{CM}}_{i\alpha,j\beta}=\boldsymbol{r}}} T_{\mu\nu}(i\alpha,j\beta)A_\nu(\boldsymbol{r},t) + j^{\mathrm{p}}_\mu(i\alpha,j\beta). \tag{D3}$$

Repeated indices are summed over. The operators $T_{\mu\nu}(i\alpha,j\beta)A_\nu = -\sum_\sigma t^\sigma_{i\alpha,j\beta}[r^{\mathrm{rel}}_{i\alpha,j\beta}]_\mu[r^{\mathrm{rel}}_{i\alpha,j\beta}]_\nu c^\dagger_{i\alpha\sigma}c_{j\beta\sigma}A_\nu$ and $j^{\mathrm{p}}_\mu(i\alpha,j\beta) = -i\sum_\sigma t^\sigma_{i\alpha,j\beta}[r^{\mathrm{rel}}_{i\alpha,j\beta}]_\mu c^\dagger_{i\alpha\sigma}c_{j\beta\sigma}$ are the diamagnetic and paramagnetic current operators, respectively.

The functional derivative of the mean field interaction Hamiltonian is

$$\frac{\delta H_{\mathrm{int}}}{\delta A_\mu} = \sum_{i\alpha} \frac{\delta\Delta_{i\alpha}}{\delta A_\mu} c^\dagger_{i\alpha\uparrow} c^\dagger_{i\alpha\downarrow} + \mathrm{H.c.} - \left(\frac{\delta\Delta_{i\alpha}}{\delta A_\mu}\frac{\Delta^*_{i\alpha}}{U} + \mathrm{H.c.}\right). \tag{D4}$$

Using the linear response approximation $\Delta_{i\alpha}(\boldsymbol{A}) \approx \Delta_{i\alpha}(\boldsymbol{A} = \boldsymbol{0}) + \delta\Delta_{i\alpha}/\delta A_\nu|_{\boldsymbol{A}=\boldsymbol{0}} A_\nu$, Eq. (D4) becomes

$$\frac{\delta H_{\mathrm{int}}}{\delta A_\mu} = \sum_{i\alpha} \frac{\delta\Delta_{i\alpha}}{\delta A_\mu} c^\dagger_{i\alpha\uparrow} c^\dagger_{i\alpha\downarrow}\bigg|_{\boldsymbol{A}=\boldsymbol{0}} + \mathrm{H.c.} - \frac{1}{U}\sum_{i\alpha}\left(\Delta^*_{i\alpha}\frac{\delta\Delta_{i\alpha}}{\delta A_\mu}\bigg|_{\boldsymbol{A}=\boldsymbol{0}} + \mathrm{H.c}\right) - \frac{1}{U}\sum_{i\alpha}\left(\frac{\delta\Delta_{i\alpha}}{\delta A_\mu}\frac{\delta\Delta^*_{i\alpha}}{\delta A_\nu}\bigg|_{\boldsymbol{A}=\boldsymbol{0}} + \mathrm{H.c.}\right)A_\nu. \tag{D5}$$

By combining Eqs. (D3) and (D5), we obtain the total current density operator

$$\langle j_\mu(\boldsymbol{r},t)\rangle = -\sum_{\substack{i\alpha,j\beta: \\ \boldsymbol{r}^{\mathrm{CM}}_{i\alpha,j\beta}=\boldsymbol{r}}} \left[\langle\widetilde{T}_{\mu\nu}(i\alpha,j\beta)\rangle A_\nu(\boldsymbol{r}^{\mathrm{CM}}_{i\alpha,j\beta},t) + \langle\widetilde{j}^{\mathrm{p}}_\mu(i\alpha,j\beta)\rangle\right], \tag{D6}$$

$$\widetilde{T}_{\mu\nu}(i\alpha,j\beta) = T_{\mu\nu}(i\alpha,j\beta) - \frac{1}{U}\left(\frac{\delta\Delta_{i\alpha}}{\delta A_\mu(\boldsymbol{r}_{i\alpha},t)}\frac{\delta\Delta^*_{i\alpha}}{\delta A_\nu(\boldsymbol{r}_{i\alpha},t)}\bigg|_{\boldsymbol{A}=\boldsymbol{0}} + \mathrm{H.c.}\right)\delta_{i\alpha,j\beta}, \tag{D7}$$

$$\widetilde{j}^{\mathrm{p}}_\mu(i\alpha,j\beta) = j^{\mathrm{p}}_\mu(i\alpha,j\beta) + \left(\frac{\delta\Delta_{i\alpha}}{\delta A_\mu(\boldsymbol{r}_{i\alpha},t)}\bigg|_{\boldsymbol{A}=\boldsymbol{0}} c^\dagger_{i\alpha\uparrow}c^\dagger_{i\alpha\downarrow} - \frac{1}{U}\frac{\delta\Delta_{i\alpha}}{\delta A_\mu(\boldsymbol{r}_{i\alpha},t)}\Delta^*_{i\alpha}\bigg|_{\boldsymbol{A}=\boldsymbol{0}} + \mathrm{H.c.}\right)\delta_{i\alpha,j\beta}. \tag{D8}$$

As $\boldsymbol{A}$ varies slowly in both space and time, we can assume the induced current has the same spatial and temporal dependence as $\boldsymbol{A}$, so that

$$\langle j_\mu(\boldsymbol{q},\omega)\rangle = -K_{\mu\nu}(\boldsymbol{q},\omega)A_\nu(\boldsymbol{q},\omega), \tag{D9}$$

where $K_{\mu\nu}$ is the current-current response function. The Fourier-transformed total current density reads as $\langle j_\mu(\boldsymbol{q},t)\rangle = (1/V)\sum_{\boldsymbol{r}}\langle j_\mu(\boldsymbol{r},t)\rangle e^{-i\boldsymbol{q}\cdot\boldsymbol{r}}$. Assuming the order parameter is uniform in each sublattice (i.e., may depend on the orbital α, but for a given orbital is the same at each unit cell i), we obtain

$$\langle j_\mu(\boldsymbol{q},t)\rangle = -\langle\widetilde{T}_{\mu\nu}\rangle A_\nu(\boldsymbol{q},t) - \langle\widetilde{j}^{\mathrm{p}}_\mu(\boldsymbol{q})\rangle, \tag{D10}$$

$$\widetilde{T}_{\mu\nu} = \frac{1}{V}\sum_{\boldsymbol{k},\sigma}\sum_{\alpha\beta}[\partial_\mu\partial_\nu H_\sigma(\boldsymbol{k}')|_{\boldsymbol{k}'=\boldsymbol{k}}]_{\alpha\beta}c^\dagger_{\boldsymbol{k}\alpha\sigma}c_{\boldsymbol{k}\beta\sigma} - \frac{1}{U}\frac{1}{V_c}\sum_\alpha\left(\frac{\delta\Delta_\alpha}{\delta A_\mu}\frac{\delta\Delta^*_\alpha}{\delta A_\nu} + \mathrm{H.c.}\right), \tag{D11}$$

$$\widetilde{j}^{\mathrm{p}}_\mu(\boldsymbol{q}) = \frac{1}{V}\sum_{\boldsymbol{k},\sigma}\sum_{\alpha\beta}[\partial_\mu H_\sigma(\boldsymbol{k}')|_{\boldsymbol{k}'=\boldsymbol{k}+\boldsymbol{q}/2}]_{\alpha\beta}c^\dagger_{\boldsymbol{k}\alpha\sigma}c_{\boldsymbol{k}+\boldsymbol{q}\beta\sigma} + \frac{1}{V}\sum_{\boldsymbol{k}\alpha}\frac{\delta\Delta_\alpha}{\delta A_\mu}c^\dagger_{\boldsymbol{k}-\boldsymbol{q}\alpha\uparrow}c^\dagger_{-\boldsymbol{k}\alpha\downarrow} + \frac{\delta\Delta^*_\alpha}{\delta A_\mu}c_{-\boldsymbol{k}\alpha\downarrow}c_{\boldsymbol{k}+\boldsymbol{q}\alpha\uparrow}$$
$$-\frac{1}{V}\sum_{\boldsymbol{r}_{i\alpha}}\frac{1}{U}\left(\frac{\delta\Delta^*_\alpha}{\delta A_\mu}\Delta_\alpha(\boldsymbol{0}) + \mathrm{H.c.}\right)e^{-i\boldsymbol{q}\cdot\boldsymbol{r}_{i\alpha}}, \tag{D12}$$

where $\delta\Delta_\alpha/\delta A_\mu = \delta\Delta_{i\alpha}/\delta A_\mu(\boldsymbol{r}_{i\alpha},t)|_{\boldsymbol{A}=\boldsymbol{0}}$ and V_c is the volume of a unit cell, $V_c = V/N_c$.

In linear response theory, the paramagnetic part can be computed using the Kubo formula

$$\langle \widetilde{j}^{\mathrm{p}}_{\mu}(\boldsymbol{q},\omega)\rangle = -iV\sum_{\nu}\int_{0}^{\infty} dt\, e^{i\omega t}\langle[\widetilde{j}^{\mathrm{p}}_{\mu}(\boldsymbol{q},t),\widetilde{j}^{\mathrm{p}}_{\nu}(-\boldsymbol{q},0)]\rangle A_{\nu}(\boldsymbol{q},\omega). \tag{D13}$$

We will compute the current-current response function $K_{\mu\nu}$ in imaginary time using the Matsubara formalism. To compute the contribution from the paramagnetic current, we define

$$\Pi_{\mu\nu}(\boldsymbol{q},\tau) = V^2\langle T[\widetilde{j}^{\mathrm{p}}_{\mu}(\boldsymbol{q},\tau)\widetilde{j}^{\mathrm{p}}_{\nu}(-\boldsymbol{q},0)]\rangle, \tag{D14}$$

where T is the imaginary-time ordering operator.

In the computation of $\Pi_{\mu\nu}$, it will be useful to define the following block matrices:

$$\widetilde{H}(\boldsymbol{k}) = \begin{pmatrix} H_{\uparrow}(\boldsymbol{k}) & \mathbf{0} \\ \mathbf{0} & -H^{*}_{\downarrow}(-\boldsymbol{k}) \end{pmatrix}, \tag{D15}$$

$$G^{\alpha\beta}(\boldsymbol{k}) = -\begin{pmatrix} \langle T[c_{\boldsymbol{k}\alpha\uparrow}(\tau)c^{\dagger}_{\boldsymbol{k}\beta\uparrow}]\rangle & \langle T[c_{\boldsymbol{k}\alpha\uparrow}(\tau)c_{-\boldsymbol{k}\beta\downarrow}]\rangle \\ \langle T[c^{\dagger}_{-\boldsymbol{k}\alpha\downarrow}(\tau)c^{\dagger}_{\boldsymbol{k}\beta\uparrow}]\rangle & \langle T[c^{\dagger}_{-\boldsymbol{k}\alpha\downarrow}(\tau)c_{-\boldsymbol{k}\beta\downarrow}]\rangle \end{pmatrix}, \tag{D16}$$

$$\delta_{\nu}\Delta = \begin{pmatrix} \mathbf{0} & \frac{\delta\boldsymbol{\Delta}}{\delta A_{\nu}} \\ \frac{\delta\boldsymbol{\Delta}^{*}}{\delta A_{\nu}} & \mathbf{0} \end{pmatrix}, \tag{D17}$$

$$\frac{\delta\boldsymbol{\Delta}}{\delta A_{\nu}} = \mathrm{diag}\left(\frac{\delta\Delta_1}{\delta A_{\nu}},\ldots,\frac{\delta\Delta_n}{\delta A_{\nu}}\right). \tag{D18}$$

We use the following indexing convention: A_{ij} designates the block (i,j), and $A^{\alpha\beta}_{ij}$ designates the component (α,β) in said block. For example, $G(\tau,\boldsymbol{k})^{\alpha\beta}_{01} = -\langle T[c_{\boldsymbol{k}\alpha\uparrow}c_{-\boldsymbol{k}\beta\downarrow}]\rangle$. For readability, we will use the notation $\partial_{\mu}A|_{\boldsymbol{k}} = \partial A(\boldsymbol{k}')/\partial k'_{\mu}|_{\boldsymbol{k}'=\boldsymbol{k}}$.

If we do not take the dependence of order parameters into account, the only terms in $\Pi_{\mu\nu}(\boldsymbol{q},\tau)$ are

$$\sum_{\boldsymbol{k}\boldsymbol{k}'\sigma\sigma'\alpha\beta\gamma\delta}[\partial_{\mu}H_{\sigma}|_{\boldsymbol{k}+\boldsymbol{q}/2}]^{\alpha\beta}[\partial_{\nu}H_{\sigma'}|_{\boldsymbol{k}'-\boldsymbol{q}/2}]^{\gamma\delta}\langle T[c^{\dagger}_{\boldsymbol{k}\alpha\sigma}(\tau)c_{\boldsymbol{k}+\boldsymbol{q}\beta\sigma}(\tau)c^{\dagger}_{\boldsymbol{k}'\gamma\sigma'}c_{\boldsymbol{k}'-\boldsymbol{q}\delta\sigma'}]\rangle. \tag{D19}$$

These can be expressed as $\Pi^{(0)}_{\mu\nu} = -\sum_{\boldsymbol{k}}\mathrm{Tr}[G(-\tau,\boldsymbol{k})\partial_{\mu}\widetilde{H}|_{\boldsymbol{k}+\boldsymbol{q}/2}\gamma^{z}G(\tau,\boldsymbol{k}+\boldsymbol{q})\partial_{\nu}\widetilde{H}|_{\boldsymbol{k}+\boldsymbol{q}/2}\gamma^{z}]$.

For the new terms related to the derivatives of the order parameters, let us start from those where the prefactor involves one derivative of Δ_{α} or Δ^{*}_{α}. We will show detailed steps for

$$\sum_{\boldsymbol{k}\boldsymbol{k}'\sigma\alpha\beta\gamma}\frac{\delta\Delta_{\alpha}}{\delta A_{\mu}}[\partial_{\nu}H_{\sigma}|_{\boldsymbol{k}'-\boldsymbol{q}/2}]^{\beta\gamma}\langle T[c^{\dagger}_{\boldsymbol{k}-\boldsymbol{q}\alpha\uparrow}(\tau)c^{\dagger}_{-\boldsymbol{k}\alpha\downarrow}(\tau)c^{\dagger}_{\boldsymbol{k}'\beta\sigma}c_{\boldsymbol{k}'-\boldsymbol{q}\gamma\sigma}]\rangle. \tag{D20}$$

Taking only one-loop graphs and ignoring disconnected ones, the four-point correlator becomes

$$\begin{aligned}
&\langle T[c^{\dagger}_{\boldsymbol{k}-\boldsymbol{q}\alpha\uparrow}(\tau)c^{\dagger}_{-\boldsymbol{k}\alpha\downarrow}(\tau)c^{\dagger}_{\boldsymbol{k}'\beta\sigma}c_{\boldsymbol{k}'-\boldsymbol{q}\gamma\sigma}]\rangle \\
&\quad = -\langle T[c^{\dagger}_{\boldsymbol{k}-\boldsymbol{q}\alpha\uparrow}(\tau)c^{\dagger}_{\boldsymbol{k}'\beta\sigma}]\rangle\langle T[c^{\dagger}_{-\boldsymbol{k}\alpha\downarrow}(\tau)c_{\boldsymbol{k}'-\boldsymbol{q}\gamma\sigma}]\rangle + \langle T[c^{\dagger}_{\boldsymbol{k}-\boldsymbol{q}\alpha\uparrow}(\tau)c_{\boldsymbol{k}'-\boldsymbol{q}\gamma\sigma}]\rangle\langle T[c^{\dagger}_{-\boldsymbol{k}\alpha\downarrow}(\tau)c^{\dagger}_{\boldsymbol{k}'\beta\sigma}]\rangle \\
&\quad = -\langle T[c^{\dagger}_{\boldsymbol{k}-\boldsymbol{q}\alpha\uparrow}(\tau)c^{\dagger}_{-\boldsymbol{k}+\boldsymbol{q}\beta\downarrow}]\rangle\langle T[c^{\dagger}_{-\boldsymbol{k}\alpha\downarrow}(\tau)c_{-\boldsymbol{k}\gamma\downarrow}]\rangle\delta_{\sigma,\downarrow}\delta_{\boldsymbol{k}',-\boldsymbol{k}+\boldsymbol{q}} + \langle T[c^{\dagger}_{\boldsymbol{k}-\boldsymbol{q}\alpha\uparrow}(\tau)c_{\boldsymbol{k}-\boldsymbol{q}\gamma\uparrow}]\rangle\langle T[c^{\dagger}_{-\boldsymbol{k}\alpha\downarrow}(\tau)c^{\dagger}_{\boldsymbol{k}\beta\uparrow}]\rangle\delta_{\sigma,\uparrow}\delta_{\boldsymbol{k}',\boldsymbol{k}}.
\end{aligned} \tag{D21}$$

Plugging this into Eq. (D20), we get from the first term

$$\begin{aligned}
&-\sum_{\boldsymbol{k}\alpha\beta\gamma}[-G^{\beta\alpha}_{10}(-\tau,\boldsymbol{k}-\boldsymbol{q})][\delta_{\mu}\Delta]^{\alpha\alpha}_{01}G^{\alpha\gamma}_{11}(\tau,\boldsymbol{k})(-[\partial_{\nu}\widetilde{H}|_{\boldsymbol{k}-\boldsymbol{q}/2}\gamma^{z}])^{\gamma\beta}_{11} \\
&\quad = -\sum_{\boldsymbol{k}\alpha\beta\gamma}G^{\beta\alpha}_{10}(-\tau,\boldsymbol{k})[\delta_{\mu}\Delta]^{\alpha\alpha}_{01}G^{\alpha\gamma}_{11}(\tau,\boldsymbol{k}+\boldsymbol{q})[\partial_{\nu}\widetilde{H}|_{\boldsymbol{k}+\boldsymbol{q}/2}\gamma^{z}]^{\gamma\beta}_{00},
\end{aligned} \tag{D22}$$

where the transformation $\boldsymbol{k}\to\boldsymbol{k}+\boldsymbol{q}$ was used. Note that

$$\partial_{\mu}\widetilde{H}|_{\boldsymbol{k}} = \begin{pmatrix} \left.\frac{\partial H_{\uparrow}(\boldsymbol{k}')}{\partial k'_{\mu}}\right|_{\boldsymbol{k}'=\boldsymbol{k}} & 0 \\ 0 & \left.\frac{\partial H^{*}_{\downarrow}(\boldsymbol{k}')}{\partial k'_{\mu}}\right|_{\boldsymbol{k}'=-\boldsymbol{k}} \end{pmatrix}. \tag{D23}$$

Similarly, the second part yields

$$\sum_{\boldsymbol{k}\alpha\beta\gamma}-G^{\gamma\alpha}_{00}(-\tau,\boldsymbol{k}-\boldsymbol{q})[\delta_{\mu}\Delta]^{\alpha\alpha}_{01}G^{\alpha\beta}_{10}(\tau,\boldsymbol{k})[\partial_{\nu}\widetilde{H}|_{\boldsymbol{k}-\boldsymbol{q}/2}]^{\beta\gamma}_{00} = -\sum_{\boldsymbol{k}\alpha\beta\gamma}G^{\gamma\alpha}_{00}(-\tau,\boldsymbol{k})[\delta_{\mu}\Delta]^{\alpha\alpha}_{01}G^{\alpha\beta}_{10}(\tau,\boldsymbol{k}+\boldsymbol{q})[\partial_{\nu}\widetilde{H}|_{\boldsymbol{k}+\boldsymbol{q}/2}]^{\beta\gamma}_{00}. \tag{D24}$$

Repeating this procedure for all terms involving one derivative of Δ or Δ^*, the total contribution is found to be

$$\Pi^{(1)}_{\mu\nu} = -\sum_{\boldsymbol{k}} \mathrm{Tr}[G(-\tau,\boldsymbol{k})\delta_\mu \Delta G(\tau,\boldsymbol{k}+\boldsymbol{q})\partial_\nu \widetilde{H}|_{\boldsymbol{k}+\boldsymbol{q}/2}\gamma^z] - \sum_{\boldsymbol{k}} \mathrm{Tr}[G(-\tau,\boldsymbol{k})\partial_\mu \widetilde{H}|_{\boldsymbol{k}+\boldsymbol{q}/2}\gamma^z G(\tau,\boldsymbol{k}+\boldsymbol{q})\delta_\nu \Delta]. \tag{D25}$$

The next contributions to the paramagnetic current come from terms which have a product of derivatives of Δ or Δ^* as a prefactor, for example,

$$\sum_{\boldsymbol{k}\boldsymbol{k}'\alpha\beta} \frac{\delta\Delta_\alpha}{\delta A_\mu}\frac{\delta\Delta_\beta}{\delta A_\nu}\langle T[c^\dagger_{\boldsymbol{k}-\boldsymbol{q}\alpha\uparrow}(\tau)c^\dagger_{-\boldsymbol{k}\alpha\downarrow}(\tau)c^\dagger_{\boldsymbol{k}'+\boldsymbol{q}\beta\uparrow}c^\dagger_{-\boldsymbol{k}'\beta\downarrow}]\rangle. \tag{D26}$$

Like before, the correlator can be expressed as

$$\begin{aligned}\langle T[c^\dagger_{\boldsymbol{k}-\boldsymbol{q}\alpha\uparrow}(\tau)c^\dagger_{-\boldsymbol{k}\alpha\downarrow}(\tau)c^\dagger_{\boldsymbol{k}'+\boldsymbol{q}\beta\uparrow}c^\dagger_{-\boldsymbol{k}'\beta\downarrow}]\rangle &= -\langle T[c^\dagger_{\boldsymbol{k}-\boldsymbol{q}\alpha\uparrow}(\tau)c^\dagger_{\boldsymbol{k}'+\boldsymbol{q}\beta\uparrow}]\rangle\langle T[c^\dagger_{-\boldsymbol{k}\alpha\downarrow}(\tau)c^\dagger_{-\boldsymbol{k}'\beta\downarrow}]\rangle \\ &\quad + \langle T[c^\dagger_{\boldsymbol{k}+\boldsymbol{q}\alpha\downarrow}(\tau)c^\dagger_{\boldsymbol{k}'+\boldsymbol{q}\beta\uparrow}]\rangle\langle T[c^\dagger_{\boldsymbol{k}-\boldsymbol{q}\alpha\uparrow}(\tau)c^\dagger_{-\boldsymbol{k}'\beta\downarrow}]\rangle \\ &= \langle T[c^\dagger_{-\boldsymbol{k}\alpha\downarrow}(\tau)c^\dagger_{\boldsymbol{k}\beta\uparrow}]\rangle\langle T[c^\dagger_{\boldsymbol{k}-\boldsymbol{q}\alpha\uparrow}(\tau)c^\dagger_{\boldsymbol{q}-\boldsymbol{k}\beta\downarrow}]\rangle\delta_{\boldsymbol{k}',\boldsymbol{k}-\boldsymbol{q}},\end{aligned} \tag{D27}$$

and the contribution to the paramagnetic term is

$$\sum_{\boldsymbol{k}\alpha\beta}[-G^{\beta\alpha}_{10}(-\tau,\boldsymbol{k}-\boldsymbol{q})][\delta_\mu\Delta]^{\alpha\alpha}_{01}G^{\alpha\beta}_{10}(\tau,\boldsymbol{k})[\delta_\nu\Delta]^{\beta\beta}_{01} = -\sum_{\boldsymbol{k}\alpha\beta} G^{\beta\alpha}_{10}(-\tau,\boldsymbol{k})[\delta_\mu\Delta]^{\alpha\alpha}_{01}G^{\alpha\beta}_{10}(\tau,\boldsymbol{k}+\boldsymbol{q})[\delta_\nu\Delta]^{\beta\beta}_{01}. \tag{D28}$$

Repeating this for the other terms, the contribution to the paramagnetic current is found to be

$$\Pi^{(2)}_{\mu\nu} = -\sum_{\boldsymbol{k}} \mathrm{Tr}[G(-\tau,\boldsymbol{k})\delta_\mu\Delta G(\tau,\boldsymbol{k}+\boldsymbol{q})\delta_\nu\Delta]. \tag{D29}$$

The last scalar term in the generalized paramagnetic current operator [Eq. (D12)] does not contribute, as it commutes with all operators.

By combining Eqs. (D25) and (D29), we obtain

$$\Pi_{\mu\nu}(\boldsymbol{q},\tau) = -\sum_{\boldsymbol{k}} \mathrm{Tr}\big[G(-\tau,\boldsymbol{k})(\partial_\mu\widetilde{H}|_{\boldsymbol{k}+\boldsymbol{q}/2}\gamma^z + \delta_\mu\Delta)G(\tau,\boldsymbol{k}+\boldsymbol{q})(\partial_\nu\widetilde{H}|_{\boldsymbol{k}+\boldsymbol{q}/2}\gamma^z + \delta_\nu\Delta)\big]. \tag{D30}$$

Fourier transforming $\Pi_{\mu\nu}$ to Matsubara space yields

$$\Pi_{\mu\nu}(\boldsymbol{q},i\omega_n) = -\int_0^\beta d\tau\, e^{i\omega_n\tau}\Pi_{\mu\nu}(\boldsymbol{q},\tau) \tag{D31}$$

$$= \frac{1}{\beta}\sum_{\boldsymbol{k}}\sum_{\Omega_n} \mathrm{Tr}[G(i\Omega_n,\boldsymbol{k})(\partial_\mu\widetilde{H}|_{\boldsymbol{k}+\boldsymbol{q}/2}\gamma^z + \delta_\mu\Delta)G(i\Omega_n+i\omega_n,\boldsymbol{k}+\boldsymbol{q})(\partial_\nu\widetilde{H}|_{\boldsymbol{k}+\boldsymbol{q}/2}\gamma^z + \delta_\nu\Delta)], \tag{D32}$$

where $\Omega_n = \pi(2n+1)/\beta$ is a fermionic Matsubara frequency and $\omega_n = 2\pi n/\beta$ is a bosonic one. Computing the diamagnetic contribution to the current is straightforward. The total current-current response function is given by

$$\begin{aligned}K_{\mu\nu}(\boldsymbol{q},i\omega_n) = &-\frac{1}{V}\frac{1}{\beta}\sum_{\boldsymbol{k}}\sum_{\Omega_m}\mathrm{Tr}[G(i\Omega_m,\boldsymbol{k})\partial_\mu\widetilde{H}|_{\boldsymbol{k}}G(i\Omega_m,\boldsymbol{k})\partial_\nu\widetilde{H}|_{\boldsymbol{k}}] \\ &+\frac{1}{V}\frac{1}{\beta}\sum_{\boldsymbol{k}}\sum_{\Omega_n}\mathrm{Tr}[G(i\Omega_m,\boldsymbol{k})(\partial_\mu\widetilde{H}|_{\boldsymbol{k}+\boldsymbol{q}/2}\gamma^z+\delta_\mu\Delta)G(i\Omega_m+i\omega_n,\boldsymbol{k}+\boldsymbol{q})(\partial_\nu\widetilde{H}|_{\boldsymbol{k}+\boldsymbol{q}/2}\gamma^z+\delta_\nu\Delta)] - \frac{1}{V_c}C\delta(\omega_n),\end{aligned} \tag{D33}$$

$$C = \frac{1}{U}\sum_\alpha \frac{\delta\Delta_\alpha}{\delta A_\mu}\frac{\delta\Delta^*_\alpha}{\delta A_\nu} + \mathrm{H.c.} \tag{D34}$$

In mean field theory, the BdG Hamiltonian can be diagonalized as $H_{\mathrm{BdG}} = \sum_a E_a|\psi_a\rangle\langle\psi_a|$, and the Green's function is

$$G(i\Omega_n,\boldsymbol{k}) = \sum_a \frac{|\psi_a\rangle\langle\psi_a|}{i\Omega_n - E_a(\boldsymbol{k})}. \tag{D35}$$

The superfluid weight then becomes

$$D_{s,\mu\nu} = \lim_{\boldsymbol{q}\to 0}\lim_{\omega\to 0} K_{\mu\nu}(\boldsymbol{q},\omega)|_{\boldsymbol{A}=\boldsymbol{0}} \tag{D36}$$

$$= \frac{1}{V}\sum_{\boldsymbol{k},a,b}\frac{n_F(E_b)-n_F(E_a)}{E_a-E_b}[\langle\psi_a|\partial_\mu\widetilde{H}_{\boldsymbol{k}}|\psi_b\rangle\langle\psi_b|\partial_\nu\widetilde{H}_{\boldsymbol{k}}|\psi_a\rangle - \langle\psi_a|(\partial_\mu\widetilde{H}_{\boldsymbol{k}}\gamma^z+\delta_\mu\Delta)|\psi_b\rangle\langle\psi_b|(\partial_\nu\widetilde{H}_{\boldsymbol{k}}\gamma^z+\delta_\nu\Delta)|\psi_a\rangle] - \frac{1}{V_c}C, \tag{D37}$$

where $n_F(E) = 1/(e^{\beta E} + 1)$ is the Fermi-Dirac distribution and the prefactor should be understood as $-\partial_E n_F(E)$ if $E_a = E_b$. The functional derivatives of the order parameters can be computed with knowledge of only the ground state at $\boldsymbol{A} = \boldsymbol{0}$, for example, by using the Hessian method presented in the main text [see Eq. (16)].

These equations are valid in general as long as $\delta\mu/\delta A_\mu|_{\boldsymbol{A}=\boldsymbol{0}} = 0$. If the derivative of the chemical potential is not zero, the above will be equivalent to $D_s = (1/V)d^2\Omega/dq_i dq_j|_{\mu,\boldsymbol{q}=\boldsymbol{0}}$, where μ is kept constant when taking the derivative. This may not be equal to $(1/V)d^2F/dq_i dq_j|_{N,\boldsymbol{q}=\boldsymbol{0}}$, where the particle number is kept constant.

APPENDIX E: EQUIVALENCE OF D_s OBTAINED FROM THE THERMODYNAMIC POTENTIAL AND LINEAR RESPONSE THEORY

In this Appendix, we will show that the definition $[D_s]_{\mu\nu} = (1/V)d^2F/dq_\mu dq_\nu|_{\boldsymbol{q}=\boldsymbol{0}}$ is equivalent to the result obtained from linear response theory $[D_s]_{\mu\nu} = \lim_{\boldsymbol{q}\to 0}\lim_{\omega\to 0} K_{\mu\nu}(\boldsymbol{q},\omega)|_{\boldsymbol{A}=\boldsymbol{0}}$, where $K_{\mu\nu}$ is the current-current response function $\langle j_\mu(\boldsymbol{q},\omega)\rangle = -K_{\mu\nu}(\boldsymbol{q},\omega)A_\nu(\boldsymbol{q},\omega)$.

When we define $[D_s]_{\mu\nu} = (1/V)d^2F/dq_\mu dq_\nu|_{\boldsymbol{q}=\boldsymbol{0}}$, the vector $\boldsymbol{q}$ is introduced in the phase of the order parameters $\Delta_{i\alpha} \to \Delta_{i\alpha}e^{2i\boldsymbol{q}\cdot\boldsymbol{r}_{i\alpha}}$. This phase can be moved to the kinetic Hamiltonian with a unitary transformation $c_{i\alpha\sigma} \to c_{i\alpha\sigma}e^{-i\boldsymbol{q}\cdot\boldsymbol{r}_{i\alpha}}$. The vector $\boldsymbol{q}$ is thus equivalent to a constant vector potential $\boldsymbol{A}$ introduced via a Peierls substitution.

The grand canonical potential is defined as $\Omega(\boldsymbol{A}) = -\beta^{-1}\ln Z(\boldsymbol{A})$, $Z(\boldsymbol{A}) = \mathrm{Tr}[e^{-\beta H(\boldsymbol{A})}]$. The term μN is included in the Hamiltonian [see Eq. (1)]. The functional derivative of Ω is

$$\frac{1}{V}\frac{\delta^2\Omega}{\delta A_\mu \delta A_\nu} = \frac{1}{VZ}\frac{\delta}{\delta A_\mu}\mathrm{Tr}\left[\frac{\delta H}{\delta A_\nu}e^{-\beta H(\boldsymbol{A})}\right] = \frac{\delta}{\delta A_\mu}\sum_\lambda K_{\nu\lambda}A_\lambda = K_{\nu\mu}. \tag{E1}$$

Thus

$$[D_s]_{\mu\nu} = \frac{1}{V}\frac{d^2F}{dA_\mu dA_\nu}\bigg|_{\boldsymbol{A}=\boldsymbol{0},N} = \frac{1}{V}\frac{d^2\Omega}{dA_\mu dA_\nu}\bigg|_{\boldsymbol{A}=\boldsymbol{0},\mu} = \lim_{\boldsymbol{q}\to\boldsymbol{0}}\lim_{\omega\to 0} K_{\mu\nu}(\boldsymbol{q},\omega), \tag{E2}$$

assuming that the chemical potential has a vanishing derivative at $\boldsymbol{A} = 0$. When taking the total derivative of F, the total particle number is kept constant, whereas for Ω, the chemical potential is kept constant.

APPENDIX F: FLAT BAND MODELS WITH A TUNED BAND TOUCHING

In Sec. VI B, we presented results for flat band models with a tuned band touching. We used the method developed in Ref. [48] to construct models where the flat band energy and eigenstates remain unchanged while the band touchings with the dispersive bands are tuned from linear to quadratic. For the kagome geometry, the model with a linear band touching is shown in Fig. 6. The Fourier-transformed kinetic Hamiltonian is

$$H_{\boldsymbol{k},\mathrm{lin,kago}} = -2i\begin{pmatrix} 0 & \sin(k_1/2) & \sin(k_2/2) \\ -\sin(k_1/2) & 0 & -\sin(k_3/2) \\ -\sin(k_2/2) & \sin(k_3/2) & 0 \end{pmatrix}, \tag{F1}$$

where $k_1 = k_x$, $k_2 = k_x/2 + \sqrt{3}k_y/2$, and $k_3 = k_x/2 - \sqrt{3}k_y/2$. The length of a unit-cell lattice vector is taken equal to 1. This model has a flat band at $E = 0$. The corresponding quadratic model is constructed so that the flat band is at the same energy and has the same Bloch functions. The obtained kinetic Hamiltonian is

$$H_{\boldsymbol{k},\mathrm{quad,kago}} = C\begin{pmatrix} \sin^2(k_1/2)+\sin^2(k_2/2) & -\sin(k_2/2)\sin(k_3/2) & \sin(k_1/2)\sin(k_3/2) \\ -\sin(k_2/2)\sin(k_3/2) & \sin^2(k_3/2)-2\sin^2(k_1/2) & -2\sin(k_1/2)\sin(k_2/2) \\ \sin(k_1/2)\sin(k_3/2) & -2\sin(k_1/2)\sin(k_2/2) & \sin^2(k_3/2)-2\sin^2(k_2/2) \end{pmatrix}. \tag{F2}$$

The constant C is chosen so that the total width of the band structure is the same as in the linear model. The obtained band structure is shown in Fig. 6(c). The total Hamiltonian with a continuously tuned band touching is $H_{\boldsymbol{k},\mathrm{kago}} = [(1-\lambda)H_{\boldsymbol{k},\mathrm{lin,kago}} + \lambda H_{\boldsymbol{k},\mathrm{quad,kago}}]/C_2(\lambda)$, where C_2 is chosen so that the total width of the band structure is independent of λ. Since both the linear and quadratic models have a flat band at $E = 0$ with the same eigenfunctions, the flat band eigenstates are identical for all λ.

For the Lieb geometry, we choose the same Lieb lattice as our linear model. In order to be able to open a band gap, we introduce the staggered hopping amplitudes used in the main text. The kinetic Hamiltonian is

$$H_{\boldsymbol{k},\mathrm{lin,Lieb}} = -2\begin{pmatrix} 0 & \cos(k_x/2)+i\eta\,\sin(k_x/2) & \cos(k_y/2)+i\eta\,\sin(k_y/2) \\ \cos(k_x/2)-i\eta\,\sin(k_x/2) & 0 & 0 \\ \cos(k_y/2)-i\eta\,\sin(k_y/2) & 0 & 0 \end{pmatrix}. \tag{F3}$$

The kinetic Hamiltonian for the corresponding quadratic model is

$$H_{\boldsymbol{k},\mathrm{quad,Lieb}} = -\frac{1}{\sqrt{2}}\begin{pmatrix} -2(1+\eta^2)-(1-\eta^2)[\cos(k_x)+\cos(k_y)] & 0 & 0 \\ 0 & 1+\eta^2+(1-\eta^2)\cos(k_x) & \Lambda(k_x,k_y,\eta) \\ 0 & \Lambda^*(k_x,k_y,\eta) & 1+\eta^2+(1-\eta^2)\cos(k_y) \end{pmatrix}, \tag{F4}$$

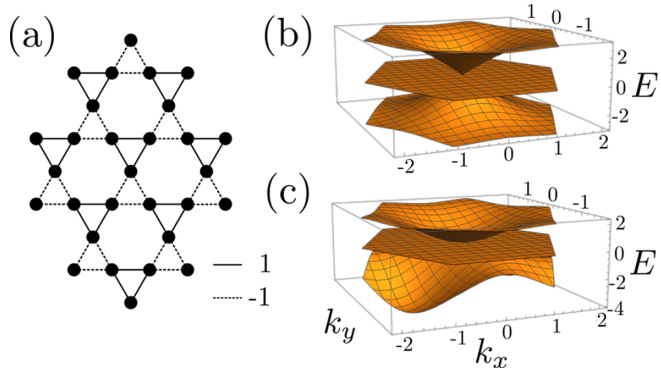

FIG. 6. (a) Schematic representation of the kagome model with a linear band touching. The corresponding band structure is shown in (b). (c) Band structure of the corresponding model with a quadratic band touching.

where $\Lambda(k_x, k_y, \eta) = 2(\cos k_x/2 - i\eta \sin k_x/2)(\cos k_y/2 + i\eta \sin k_y/2)$. One sublattice is disconnected from the others in this model. In this case, fixing the phase of one order parameter is not sufficient to make the Hessian matrix invertible, and we need to fix the overall phase in both the disconnected sublattice and the remaining two-band model. The total interpolating Hamiltonian is obtained the same way as for the kagome lattice. In this case, at $\eta = 0$, the band touching is tuned continuously from a linear to a quadratic one. For nonzero η, a gap is opened. In this case, tuning λ modifies the dispersive bands without affecting the geometry of the flat band.

APPENDIX G: *S*-MATRIX CONSTRUCTION

The S-matrix bipartite Hamiltonians [44] offer a route to understanding the mean field gap in flat band systems, even those with band-touching points. Denote the two sublattices $L, \tilde{L}$ with $N_L > N_{\tilde{L}}$, where $N_L, N_{\tilde{L}}$ are the number of orbitals per unit cell of each sublattice [44]. The kinetic energy Hamiltonian reads as

$$H_{\boldsymbol{k}} = \begin{bmatrix} 0 & S_{\boldsymbol{k}}^\dagger \\ S_{\boldsymbol{k}} & 0 \end{bmatrix}. \tag{G1}$$

Here $S_{\boldsymbol{k}}^\dagger$ is an $(N_{\tilde{L}} \times N_L)$-dimensional matrix, and so has an $(N_L - N_{\tilde{L}})$-dimensional null space that forms the flat bands. This Hamiltonian obeys a chiral symmetry

$$S = \begin{bmatrix} I_{\tilde{L}\times\tilde{L}} & 0 \\ 0 & -I_{L\times L} \end{bmatrix}, \quad \{S, H_{\boldsymbol{k}}\} = 0, \tag{G2}$$

and the dispersive and flat wave functions read as

$$\Psi^{\text{disp}}_{\boldsymbol{k},m,\pm} = \frac{1}{\sqrt{2}} \begin{bmatrix} \phi_{\boldsymbol{k},m} \\ \pm\psi_{\boldsymbol{k},m} \end{bmatrix}, \quad \Psi^{\text{flat}}_{\boldsymbol{k},n} = \begin{bmatrix} 0 \\ \psi_{\boldsymbol{k},n} \end{bmatrix}. \tag{G3}$$

Here $\phi_{\boldsymbol{k},m}$ and $\psi_{\boldsymbol{k},m}$ are normalized column vectors whose components correspond the orbitals in the $\tilde{L}$ and L sublattices, respectively. The vector $\phi_{\boldsymbol{k},m}$ has length $N_{\tilde{L}}$, and $\psi_{\boldsymbol{k},m}$ has length N_L. The dispersive states have energy $\pm\epsilon_{\boldsymbol{k},m}$, where $\epsilon_{\boldsymbol{k},m}$ are the singular values of $S_{\boldsymbol{k}}$. Due to chiral symmetry, the ϕ and ψ sublattice vectors obey their own orthonormality relations and one may define the sublattice projectors as

$$P^{\tilde{L}}_m(\boldsymbol{k}) = \phi_{\boldsymbol{k},m}\phi^\dagger_{\boldsymbol{k},m}, \; P^{L}_m(\boldsymbol{k}) = \psi_{\boldsymbol{k},m}\psi^\dagger_{\boldsymbol{k},m}, \tag{G4}$$

where $P^{\tilde{L}}_m(\boldsymbol{k})$ is an $(\tilde{L} \times \tilde{L})$-dimensional matrix, running over the orbitals α in the smaller sublattice $\tilde{L}$, and $P^{L}_m(\boldsymbol{k})$ is an $(L \times L)$-dimensional matrix, running over the orbitals α in the larger sublattice L. We allow the index m to run over *both* the $N_{\tilde{L}}$ positive-energy dispersive bands and the $N_L - N_{\tilde{L}}$ flat bands. Because there is no weight of the wave function in the smaller sublattice $\tilde{L}$ in the flat bands, $P^{\tilde{L}}_m(\boldsymbol{k}) = 0$ for m in the flat bands. The sublattice projectors satisfy

$$\text{Tr}\big[P^{\tilde{L}}_m(\boldsymbol{k})\big] = \begin{cases} 0 & \text{if } m \in \text{flat bands}, \\ 1 & \text{if } m \in \text{dispersive bands}, \end{cases} \tag{G5}$$

$$\text{Tr}\big[P^{L}_m(\boldsymbol{k})\big] = 1. \tag{G6}$$

These projectors are Hermitian and square to themselves, as expected.

Linear and quadratic band touchings

The S-matrix Hamiltonian lends itself naturally to construct models with linear band touchings at high-symmetry momenta [44], and the quadratic band touchings can be derived in a simple manner. Consider the new Hamiltonian

$$H_{\text{quad}} = \begin{bmatrix} -S_{\boldsymbol{k}}^\dagger S_{\boldsymbol{k}} & 0 \\ 0 & S_{\boldsymbol{k}} S_{\boldsymbol{k}}^\dagger \end{bmatrix}, \tag{G7}$$

where $S_{\boldsymbol{k}} S_{\boldsymbol{k}}^\dagger$ is the line graph derived from $L, \tilde{L}$ [44]. If $H_{\boldsymbol{k}}$ has a linear band-touching point, then H_{quad} has quadratic band touchings. While the flat band wave functions of H_{quad} are the same as $H_{\boldsymbol{k}}$, the dispersive wave functions change. This quadratic construction is precisely the construction employed in the Lieb lattice quadratic band-touching point discussed in Appendix F. While the quadratic band-touching point breaks chiral symmetry, the wave functions are still expressed in terms of the sublattice vectors ϕ, ψ, allowing for a precise treatment of the self-consistent mean field gap equations.

APPENDIX H: *S*-MATRIX MEAN FIELD THEORY

Adding the Hubbard interaction to the S matrix and performing a mean field analysis yields the BdG Hamiltonian

$$H_{\text{MF}} = \sum_{\boldsymbol{k},\sigma,\alpha\beta} [H_{\boldsymbol{k}}]_{\alpha\beta} c^\dagger_{\boldsymbol{k},\alpha,\sigma} c_{\boldsymbol{k},\beta,\sigma} + \sum_{\boldsymbol{k},\alpha} \Delta_\alpha c^\dagger_{\boldsymbol{k},\alpha,\uparrow} c^\dagger_{-\boldsymbol{k},\alpha,\downarrow} + \text{H.c.}, \tag{H1}$$

where

$$\Delta_{\boldsymbol{R}\alpha} = U \langle c_{\boldsymbol{R},\alpha,\downarrow} c_{\boldsymbol{R},\alpha,\uparrow} \rangle = \Delta_\alpha, \tag{H2}$$

with the Hubbard interaction parameter $U < 0$, translation invariance in $\Delta_{\boldsymbol{R}\alpha} = \Delta_\alpha$, and $\text{U}(1)_z$-spin conservation and time-reversal symmetry. Further, we assume uniform pairing within each sublattice: $\Delta_\alpha = \Delta_L$ or $\Delta_{\tilde{L}}$ depending on the sublattice α belongs to. Such a condition may be enforced by symmetries that relate each orbital within each sublattice [38].

1. Linear band touching (with chiral symmetry)

Using the nonredundant BdG basis the Hamiltonian is expressed as

$$H_{\boldsymbol{k}}^{\mathrm{BdG}} = \begin{bmatrix} 0 & S_{\boldsymbol{k}}^{\dagger} & \Delta_{\tilde{L}} I_{\tilde{L}\times\tilde{L}} & 0 \\ S_{\boldsymbol{k}} & 0 & 0 & \Delta_L I_{L\times L} \\ \Delta_{\tilde{L}} I_{\tilde{L}\times\tilde{L}} & 0 & 0 & -S_{\boldsymbol{k}}^{\dagger} \\ 0 & \Delta_L I_{L\times L} & -S_{\boldsymbol{k}} & 0 \end{bmatrix}. \quad \text{(H3)}$$

The BdG Hamiltonian possesses a chiral symmetry arising from the product of TRS and particle hole. There is another chiral symmetry inherited from the bipartite lattice. The product of these two symmetries yields a unitary symmetry.

This Hamiltonian can be solved exactly and the positive energy eigenvalues read as

$$E_{\boldsymbol{k},m}^{1,2} = \tfrac{1}{2}\big[\pm(\Delta_{\tilde{L}} - \Delta_L) + \sqrt{(\Delta_{\tilde{L}} + \Delta_L)^2 + 4\epsilon_{\boldsymbol{k},m}^2}\big]. \quad \text{(H4)}$$

In the situation where m is a flat band,

$$E_{\boldsymbol{k},m} = \Delta_L. \quad \text{(H5)}$$

If the kinetic Hamiltonian possesses a band-touching point arising from symmetry, the degeneracy between the flat bands and dispersive bands will be made manifest in the BdG spectrum. Assume that at high-symmetry momentum $\boldsymbol{K}$, the flat bands and band-touching points transform under representation $X \oplus Y$, where X is the representation induced by orbitals in the L sublattice, and Y the representation induced by orbitals in the $\tilde{L}$ sublattice. The dimensions obey $\dim(X) - \dim(Y) = N_L - N_{\tilde{L}}$, $\dim(Y) > 0$. When pairing is added, those bands transforming under irrep X gain energy $\pm\Delta_L$, and there are $\dim(Y)$ bands in addition to the flat bands that are degenerate. These new band-touching points are quadratic.

2. Quadratic band touching (no chiral symmetry)

The quadratic band-touching Hamiltonian (G7) no longer possesses chiral symmetry, but it does factor into sublattices $\tilde{L}$, L. This is true even when pairing is added:

$$H_{\mathrm{quad}}^{\mathrm{BdG}} = \begin{bmatrix} -S_{\boldsymbol{k}}^{\dagger} S_{\boldsymbol{k}} & 0 & \Delta_{\tilde{L}} I_{\tilde{L}\times\tilde{L}} & 0 \\ 0 & S_{\boldsymbol{k}} S_{\boldsymbol{k}}^{\dagger} & 0 & \Delta_L I_{L\times L} \\ \Delta_{\tilde{L}} I_{\tilde{L}\times\tilde{L}} & 0 & S_{\boldsymbol{k}}^{\dagger} S_{\boldsymbol{k}} & 0 \\ 0 & \Delta_L I_{L\times L} & 0 & -S_{\boldsymbol{k}} S_{\boldsymbol{k}}^{\dagger} \end{bmatrix}. \quad \text{(H6)}$$

Thus, each sublattice may be treated separately. The positive-energy eigenvalues are

$$E_{\boldsymbol{k},m,\tilde{L}} = \sqrt{\epsilon_{\boldsymbol{k},m}^4 + \Delta_{\tilde{L}}^2}, \quad E_{\boldsymbol{k},m,L} = \sqrt{\epsilon_{\boldsymbol{k},m}^4 + \Delta_L^2}, \quad \text{(H7)}$$

Although chiral symmetry no longer holds, this quadratic Hamiltonian still possesses the band-touching point at energy $\pm\Delta_L$.

APPENDIX I: GAP EQUATION

1. Chiral-symmetric Hamiltonian

For the chiral-symmetric Hamiltonian $H_{\boldsymbol{k}}$, the gap equation at zero temperature [5] reads as

$$\Delta_\alpha = \frac{|U|}{N}\sum_{\boldsymbol{k},m} \frac{\Delta_L + \Delta_{\tilde{L}}}{2\sqrt{(\Delta_L + \Delta_{\tilde{L}})^2 + 4\epsilon_{\boldsymbol{k},m}^2}} \times \left[P_m^{(L)}(\boldsymbol{k}) \oplus P_m^{(\tilde{L})}(\boldsymbol{k})\right]_{\alpha\alpha}. \quad \text{(I1)}$$

Employing the trace relations (G6) removes the projectors and all wave-function dependence, yielding gap equations

$$N_L \Delta_L = \frac{|U| N_{\tilde{L}}}{2} f(\Delta) + \frac{|U|(N_L - N_{\tilde{L}})}{2}, \quad \text{(I2)}$$

$$N_{\tilde{L}} \Delta_{\tilde{L}} = \frac{|U| N_{\tilde{L}}}{2} f(\Delta), \quad \text{(I3)}$$

where we have defined

$$f(\Delta) = \frac{1}{N N_{\tilde{L}}} \sum_{\boldsymbol{k},m\in\mathrm{disp}} \frac{\Delta}{\sqrt{\Delta^2 + \epsilon_{\boldsymbol{k},m}^2}}, \quad \text{(I4)}$$

$$\Delta = \frac{1}{2}(\Delta_L + \Delta_{\tilde{L}}). \quad \text{(I5)}$$

This leads to the *universal* relation

$$N_L \Delta_L - N_{\tilde{L}} \Delta_{\tilde{L}} = \frac{|U|(N_L - N_{\tilde{L}})}{2}, \quad \text{(I6)}$$

where we recognize the right-hand side of this weighted difference equation as the strength of pairing arising from the flat bands. This equation is universal as it only requires the bipartite nature of the underlying model, and does not depend on the dispersion or wave functions, nor the presence or absence of band-touching points. We have verified the weighted difference relation numerically, and the relation has been seen to hold in the Lieb lattice [7].

Further bounds on Δ_L, $\Delta_{\tilde{L}}$ can be proven by noting that $f(\Delta)$ is monotonically increasing in Δ and ranges from 0 to 1. The gap equation for the average pairing gap Δ reads as

$$\frac{\Delta}{U} = \frac{1}{4}(1 + r) f(\Delta) + \frac{1}{4}(1 - r), \; r = \frac{N_{\tilde{L}}}{N_L} \quad \text{(I7)}$$

which only depends on the average form of the dispersive bands $f(\Delta)$ and the ratio of the sublattice orbital numbers r. This equation always has a solution, as the right-hand side is positive and bounded. As $0 < f(\Delta) < 1$, the average pairing obeys

$$\frac{1}{4}(1 - r) < \frac{\Delta}{|U|} < \frac{1}{2}. \quad \text{(I8)}$$

The pairing on the L sublattice is always larger than the pairing on the $\tilde{L}$ sublattice $\Delta_L > \Delta_{\tilde{L}}$:

$$\frac{\Delta_L}{|U|} - \frac{\Delta_{\tilde{L}}}{|U|} = \frac{1}{2}(1 - r)[1 - f(\Delta)] > 0. \quad \text{(I9)}$$

The larger pairing Δ_L is maximized when $r \to 0$, or if the ratio of flat bands to dispersive bands is made as large as possible. Because there is a solution $\Delta > 0$, it follows from the self-consistent equations that $\Delta_L, \Delta_{\tilde{L}} > 0$, i.e., there is

pairing on both sublattices:

$$\Delta_{\tilde{L}} > 0,\ \Delta_L = \frac{|U|}{2}(1-r) + r\Delta_{\tilde{L}}. \tag{I10}$$

2. Quadratic band touching

The gap equations for the quadratic Hamiltonian decouple into $\tilde{L}, L$ sectors. Defining

$$f^{\text{quad}}(\Delta) = \frac{1}{NN_{\tilde{L}}} \sum_{m\in\text{disp}} \sum_{\boldsymbol{k}} \frac{\Delta}{\sqrt{\Delta^2 + \epsilon_{\boldsymbol{k},m}^4}}, \tag{I11}$$

the self-consistent equations read as

$$\Delta_{\tilde{L}} = \frac{|U|}{2} f^{\text{quad}}(\Delta_{\tilde{L}}), \tag{I12}$$

$$\Delta_L = \frac{|U|}{2} r f^{\text{quad}}(\Delta_L) + \frac{|U|}{2}(1-r). \tag{I13}$$

As in the linear case, this system always has at least one solution: $\Delta_{\tilde{L}} = 0$ satisfies the first equation and the second always has a solution as $f^{\text{quad}}(\Delta_L)$ is bounded.

The universal relation for the chiral Hamiltonians no longer holds (as the quadratic band-touching model does not obey the chiral symmetry): instead, the weighted difference reads as

$$N_L\Delta_L - N_{\tilde{L}}\Delta_{\tilde{L}} = \frac{|U|N_{\tilde{L}}}{2}[f^{\text{quad}}(\Delta_L) - f^{\text{quad}}(\Delta_{\tilde{L}})] + \frac{|U|(N_L - N_{\tilde{L}})}{2}. \tag{I14}$$

If $\Delta_L > \Delta_{\tilde{L}}$, then regardless of the form of f^{quad}, the weighted pairing difference $N_L\Delta_L - N_{\tilde{L}}\Delta_{\tilde{L}}$ increases from the linear model to the quadratic model. In the linear model it is clear that $\Delta_L > \Delta_{\tilde{L}}$, and if $\Delta_{\tilde{L}} = 0$ in the quadratic model, the inequality is also obvious.

Unfortunately, one cannot make the general claim that $\Delta_L > \Delta_{\tilde{L}}$. Although we expect $\Delta_L > \Delta_{\tilde{L}}$ as the flat bands contribute to the superconductivity in Δ_L but not $\Delta_{\tilde{L}}$, we can only prove the slightly weaker statement: if there is a self-consistent solution $\Delta_{\tilde{L}}$, there is also a self-consistent solution Δ_L where $\Delta_L > \Delta_{\tilde{L}}$. To prove this, define the functions

$$u(\Delta) = \frac{|U|}{2} f^{\text{quad}}(\Delta), \tag{I15}$$

$$v(\Delta) = \frac{|U|}{2} r f^{\text{quad}}(\Delta) + \frac{|U|}{2}(1-r), \tag{I16}$$

and as such $0 < u(\Delta) < v(\Delta) < \frac{|U|}{2}$. Assume the fixed point $u(\Delta_{\tilde{L}}) = \Delta_{\tilde{L}}$. Because $u(\Delta) < v(\Delta)$, we have

$$\Delta_{\tilde{L}} - v(\Delta_{\tilde{L}}) < \Delta_{\tilde{L}} - u(\Delta_{\tilde{L}}) = 0\,. \tag{I17}$$

But note that the function $\Delta - v(\Delta)$ also attains positive value by setting $\Delta = |U|/2 + \epsilon,\ \epsilon > 0$, and using $v(\Delta) < |U|/2$. By the intermediate value theorem, there exists $\Delta_L \in (\Delta_{\tilde{L}}, |U|/2)$ such that $\Delta_L - v(\Delta_L) = 0$. Hence, we have demonstrated a solution exists to Eq. (I13) where $\Delta_L > \Delta_{\tilde{L}}$. This establishes that there exists a self-consistent solution of Eq. (I13) where $\Delta_L > \Delta_{\tilde{L}}$ and thus $N_L\Delta_L - N_{\tilde{L}}\Delta_{\tilde{L}}$ increases in the quadratic band-touching case relative to the linear band-touching case, though this is due to the nature of the dispersive band wave functions and not the dispersion.

We emphasize that the universal relations between Δ_L, $\Delta_{\tilde{L}}$ we have derived arise due to the geometry of the bipartite wave functions, and not due to the dispersion. This is a striking result of the bipartite S-matrix construction: various inequalities regarding the strength of the pairing gap can be made without recourse to the details of the model. The details, however, do affect the physics: tuning the band-touching point to be quadratic should enhance the gap Δ_L, as the quadratic band structure has greater density of states at low energy, increasing $f(\Delta)$.

3. Connection to Lieb's theorem and the uniform pairing models

One can connect our mean field results to the models studied by Refs. [33,69–71]. In his seminal paper, Lieb proved that the ground state of a bipartite lattice with onsite attractive interactions, assuming appropriate symmetries, is unique. If the flat bands are gapped from the dispersive bands, one can project away the dispersive bands and further argue that the ground state takes the form of the BCS wave function [7] (this is not necessarily true if there are band-touching points). Because the dispersive bands have been projected away, there is no weight of the flat bands in the smaller sublattice, so $\Delta_{\tilde{L}} = 0$. Our mean field results yield a particularly simple result in this projected limit: if the dispersive bands are sufficiently gapped from the flat bands, $f(\Delta) \to 0$, and the pairings in the sublattices read as

$$\Delta_{\tilde{L}} = 0,\ \ \Delta_L = \frac{|U|(N_L - N_{\tilde{L}})}{2N_L}. \tag{I18}$$

The strength of the pairing Δ_L is universal and does not depend on the form of the wave functions.

[1] T. T. Heikkilä, N. B. Kopnin, and G. E. Volovik, Flat bands in topological media, JETP Lett. **94**, 233 (2011).

[2] V. A. Khodel' and V. R. Shaginyan, Superfluidity in system with fermion condensate, Pis'ma Zh. Eksp. Teor. Fiz. **51**, 488 (1990) [Sov. J. Exp. Theor. Phys. Lett. **51**, 553 (1990)].

[3] N. B. Kopnin, T. T. Heikkilä, and G. E. Volovik, High-temperature surface superconductivity in topological flat-band systems, Phys. Rev. B **83**, 220503(R) (2011).

[4] D. J. Scalapino, S. R. White, and S. Zhang, Insulator, metal, or superconductor: The criteria, Phys. Rev. B **47**, 7995 (1993).

[5] S. Peotta and P. Törmä, Superfluidity in topologically nontrivial flat bands, Nat. Commun. **6**, 8944 (2015).

[6] L. Liang, T. I. Vanhala, S. Peotta, T. Siro, A. Harju, and P. Törmä, Band geometry, Berry curvature, and superfluid weight, Phys. Rev. B **95**, 024515 (2017).

[7] A. Julku, S. Peotta, T. I. Vanhala, D.-H. Kim, and P. Törmä, Geometric Origin of Superfluidity in the Lieb-Lattice Flat Band, Phys. Rev. Lett. **117**, 045303 (2016).

[8] E. Rossi, Quantum metric and correlated states in two-dimensional systems, Curr. Opin. Solid State Mater. Sci. **25**, 100952 (2021).

[9] J. P. Provost and G. Vallee, Riemannian structure on manifolds of quantum states, Commun. Math. Phys. **76**, 289 (1980).

[10] R. Resta, The insulating state of matter: A geometrical theory, Eur. Phys. J. B **79**, 121 (2011).

[11] T. Ozawa and N. Goldman, Extracting the quantum metric tensor through periodic driving, Phys. Rev. B **97**, 201117(R) (2018).

[12] J. S. Hofmann, E. Berg, and D. Chowdhury, Superconductivity, pseudogap, and phase separation in topological flat bands, Phys. Rev. B **102**, 201112(R) (2020).

[13] J. Herzog-Arbeitman, V. Peri, F. Schindler, S. D. Huber, and B. A. Bernevig, Superfluid Weight Bounds from Symmetry and Quantum Geometry in Flat Bands, Phys. Rev. Lett. **128**, 087002 (2022).

[14] V. Peri, Z.-D. Song, B. A. Bernevig, and S. D. Huber, Fragile Topology and Flat-Band Superconductivity in the Strong-Coupling Regime, Phys. Rev. Lett. **126**, 027002 (2021).

[15] Y. Cao, V. Fatemi, S. Fang, K. Watanabe, T. Taniguchi, E. Kaxiras, and P. Jarillo-Herrero, Unconventional superconductivity in magic-angle graphene superlattices, Nature (London) **556**, 43 (2018).

[16] Y. Cao, V. Fatemi, A. Demir, S. Fang, S. L. Tomarken, J. Y. Luo, J. D. Sanchez-Yamagishi, K. Watanabe, T. Taniguchi, E. Kaxiras, R. C. Ashoori, and P. Jarillo-Herrero, Correlated insulator behaviour at half-filling in magic-angle graphene superlattices, Nature (London) **556**, 80 (2018).

[17] M. Yankowitz, S. Chen, H. Polshyn, Y. Zhang, K. Watanabe, T. Taniguchi, D. Graf, A. F. Young, and C. R. Dean, Tuning superconductivity in twisted bilayer graphene, Science **363**, 1059 (2019).

[18] J. M. Park, Y. Cao, K. Watanabe, T. Taniguchi, and P. Jarillo-Herrero, Tunable strongly coupled superconductivity in magic-angle twisted trilayer graphene, Nature (London) **590**, 249 (2021).

[19] C. Shen, Y. Chu, Q. Wu, N. Li, S. Wang, Y. Zhao, J. Tang, J. Liu, J. Tian, K. Watanabe, T. Taniguchi, R. Yang, Z. Y. Meng, D. Shi, O. V. Yazyev, and G. Zhang, Correlated states in twisted double bilayer graphene, Nat. Phys. **16**, 520 (2020).

[20] Y. Cao, D. Rodan-Legrain, O. Rubies-Bigorda, J. M. Park, K. Watanabe, T. Taniguchi, and P. Jarillo-Herrero, Tunable correlated states and spin-polarized phases in twisted bilayer-bilayer graphene, Nature (London) **583**, 215 (2020).

[21] L. Balents, C. R. Dean, D. K. Efetov, and A. F. Young, Superconductivity and strong correlations in moiré flat bands, Nat. Phys. **16**, 725 (2020).

[22] E. Y. Andrei, D. K. Efetov, P. Jarillo-Herrero, A. H. MacDonald, K. F. Mak, T. Senthil, E. Tutuc, A. Yazdani, and A. F. Young, The marvels of moiré materials, Nat. Rev. Mater. **6**, 201 (2021).

[23] F. Xie, Z. Song, B. Lian, and B. A. Bernevig, Topology-Bounded Superfluid Weight in Twisted Bilayer Graphene, Phys. Rev. Lett. **124**, 167002 (2020).

[24] A. Julku, T. J. Peltonen, L. Liang, T. T. Heikkilä, and P. Törmä, Superfluid weight and Berezinskii-Kosterlitz-Thouless transition temperature of twisted bilayer graphene, Phys. Rev. B **101**, 060505(R) (2020).

[25] X. Hu, T. Hyart, D. I. Pikulin, and E. Rossi, Geometric and Conventional Contribution to the Superfluid Weight in Twisted Bilayer Graphene, Phys. Rev. Lett. **123**, 237002 (2019).

[26] P. Törmä, S. Peotta, and B. A. Bernevig, Superconductivity, superfluidity and quantum geometry in twisted multilayer systems, Nat. Rev. Phys. (2022), doi:10.1038/s42254-022-00466-y.

[27] H. Tian, S. Che, T. Xu, P. Cheung, K. Watanabe, T. Taniguchi, M. Randeria, F. Zhang, C. N. Lau, and M. W. Bockrath, Evidence for flat band Dirac superconductor originating from quantum geometry, arXiv:2112.13401.

[28] S. M. Chan, B. Grémaud, and G. G. Batrouni, Pairing and superconductivity in quasi-one-dimensional flat-band systems: Creutz and sawtooth lattices, Phys. Rev. B **105**, 024502 (2022).

[29] I. Esterlis, B. Nosarzewski, E. W. Huang, B. Moritz, T. P. Devereaux, D. J. Scalapino, and S. A. Kivelson, Breakdown of the Migdal-Eliashberg theory: A determinant quantum Monte Carlo study, Phys. Rev. B **97**, 140501(R) (2018).

[30] I. Esterlis, S. A. Kivelson, and D. J. Scalapino, A bound on the superconducting transition temperature, npj Quantum Mater. **3**, 59 (2018).

[31] E. Taylor, A. Griffin, N. Fukushima, and Y. Ohashi, Pairing fluctuations and the superfluid density through the BCS-BEC crossover, Phys. Rev. A **74**, 063626 (2006).

[32] S. H. Simon and M. S. Rudner, Contrasting lattice geometry dependent versus independent quantities: Ramifications for Berry curvature, energy gaps, and dynamics, Phys. Rev. B **102**, 165148 (2020).

[33] M. Tovmasyan, S. Peotta, P. Törmä, and S. D. Huber, Effective theory and emergent SU (2) symmetry in the flat bands of attractive Hubbard models, Phys. Rev. B **94**, 245149 (2016).

[34] M. Iskin, Origin of flat-band superfluidity on the Mielke checkerboard lattice, Phys. Rev. A **99**, 053608 (2019).

[35] G. Orso and M. Singh, Pairs, trimers, and BCS-BEC crossover near a flat band Sawtooth lattice, Phys. Rev. B, **106**, 014504 (2022).

[36] P. Törmä, L. Liang, and S. Peotta, Quantum metric and effective mass of a two-body bound state in a flat band, Phys. Rev. B **98**, 220511(R) (2018).

[37] M. Iskin, Two-body problem in a multiband lattice and the role of quantum geometry, Phys. Rev. A **103**, 053311 (2021).

[38] J. Herzog-Arbeitman, A. Chew, K.-E. Huhtinen, P. Törmä, and B. A. Bernevig (unpublished).

[39] H. Aoki, Theoretical possibilities for flat band superconductivity, J. Supercond. Novel Magn. **33**, 2341 (2020).

[40] K. Kuroki, T. Higashida, and R. Arita, High-T_c superconductivity due to coexisting wide and narrow bands: A fluctuation exchange study of the Hubbard ladder as a test case, Phys. Rev. B **72**, 212509 (2005).

[41] K. Kobayashi, M. Okumura, S. Yamada, M. Machida, and H. Aoki, Superconductivity in repulsively interacting fermions on a diamond chain: Flat-band-induced pairing, Phys. Rev. B **94**, 214501 (2016).

[42] K. Matsumoto, D. Ogura, and K. Kuroki, Wide applicability of high-T_c pairing originating from coexisting wide and incipient narrow bands in quasi-one-dimensional systems, Phys. Rev. B **97**, 014516 (2018).

[43] Y.-R. Wu, X.-F. Zhang, C.-F. Liu, W.-M. Liu, and Y.-C. Zhang, Superfluid density and collective modes of fermion superfluid in dice lattice, Sci. Rep. **11**, 13572 (2021).

[44] D. Calugaru, A. Chew, L. Elcoro, Y. Xu, N. Regnault, Z.-D. Song, and B. A. Bernevig, General construction and

topological classification of crystalline flat bands, Nat. Phys. **18**, 185 (2022).

[45] V. L. Berezinsky, Destruction of long range order in one-dimensional and two-dimensional systems having a continuous symmetry group. I. Classical systems, Zh. Eksp. Teor. Fiz. **59**, 907 (1971) [Sov. Phys.–JETP **32**, 493 (1971)].

[46] J. M. Kosterlitz and D. J. Thouless, Ordering, metastability and phase transitions in two-dimensional systems, J. Phys. C: Solid State Phys. **6**, 1181 (1973).

[47] D. R. Nelson and J. M. Kosterlitz, Universal Jump in the Superfluid Density of Two-Dimensional Superfluids, Phys. Rev. Lett. **39**, 1201 (1977).

[48] A. Graf and F. Piéchon, Designing flat-band tight-binding models with tunable multifold band touching points, Phys. Rev. B **104**, 195128 (2021).

[49] N. Regnault, Y. Xu, M.-R. Li, D.-S. Ma, M. Jovanovic, A. Yazdani, S. S. P. Parkin, C. Felser, L. M. Schoop, N. P. Ong, R. J. Cava, L. Elcoro, Z.-D. Song, and B. A. Bernevig, Catalogue of flat-band stoichiometric materials, Nature (London) **603**, 824 (2022).

[50] M. Iskin, Superfluid stiffness for the attractive Hubbard model on a honeycomb optical lattice, Phys. Rev. A **99**, 023608 (2019).

[51] T. Kitamura, T. Yamashita, J. Ishizuka, A. Daido, and Y. Yanase, Superconductivity in Monolayer FeSe Enhanced by Quantum Geometry, Phys. Rev. Research, **4**, 023232 (2022).

[52] T. J. Peltonen and T. T. Heikkil, Flat-band superconductivity in Periodically Strained Graphene: Mean-field and Berezinskii–Kosterlitz–Thouless transition, J. Phys.: Condens. Matter **32**, 365603 (2020).

[53] A. Lau, S. Peotta, D. I. Pikulin, E. Rossi, and T. Hyart, Universal suppression of superfluid weight by disorder independent of quantum geometry and band dispersion, arXiv:2203.01058.

[54] N. Verma, T. Hazra, and M. Randeria, Optical spectral weight, phase stiffness, and Tc bounds for trivial and topological flat band superconductors, Proc. Natl. Acad. Sci. USA **118**, e2106744118 (2021).

[55] A. Julku, G. M. Bruun, and P. Törmä, Quantum Geometry and Flat band Bose-Einstein Condensation, Phys. Rev. Lett. **127**, 170404 (2021).

[56] A. Julku, G. M. Bruun, and P. Törmä, Excitations of a Bose-Einstein condensate and the quantum geometry of a flat band, Phys. Rev. B **104**, 144507 (2021).

[57] M. Iskin, Effective-mass tensor of the two-body bound states and the quantum-metric tensor of the underlying Bloch states in multiband lattices, Phys. Rev. A **105**, 023312 (2022).

[58] J. Mitscherling and T. Holder, Bound on resistivity in flat-band materials due to the quantum metric, Phys. Rev. B **105**, 085154 (2022).

[59] F. Piéchon, A. Raoux, J.-N. Fuchs, and G. Montambaux, Geometric orbital susceptibility: Quantum metric without Berry curvature, Phys. Rev. B **94**, 134423 (2016).

[60] Y. Gao, S. A. Yang, and Q. Niu, Geometrical effects in orbital magnetic susceptibility, Phys. Rev. B **91**, 214405 (2015).

[61] M. Iskin, Geometric contribution to the Goldstone mode in spinorbit coupled fermi superfluids, Phys. B (Amsterdam) **592**, 412260 (2020).

[62] A. Abouelkomsan, K. Yang, and E. J. Bergholtz, Quantum metric induced phases in moiré materials, arXiv:2202.10467.

[63] Y. Gao and D. Xiao, Nonreciprocal Directional Dichroism Induced by the Quantum Metric Dipole, Phys. Rev. Lett. **122**, 227402 (2019).

[64] T. Holder, D. Kaplan, and B. Yan, Consequences of time-reversal-symmetry breaking in the light-matter interaction: Berry curvature, quantum metric, and diabatic motion, Phys. Rev. Research **2**, 033100 (2020).

[65] J. Ahn, G.-Y. Guo, N. Nagaosa, and A. Vishwanath, Riemannian geometry of resonant optical responses, Nat. Phys. **18**, 290 (2022).

[66] J. Mitscherling, Longitudinal and anomalous Hall conductivity of a general two-band model, Phys. Rev. B **102**, 165151 (2020).

[67] Y.-P. Lin and W.-H. Hsiao, Dual Haldane sphere and quantized band geometry in chiral multifold fermions, Phys. Rev. B **103**, L081103 (2021).

[68] Y.-P. Lin and W.-H. Hsiao, Band geometry from position-momentum duality at topological band crossings, Phys. Rev. B **105**, 075127 (2022).

[69] E. H. Lieb, Two Theorems on the Hubbard Model, Phys. Rev. Lett. **62**, 1201 (1989).

[70] A. Mielke, Exact ground states for the Hubbard model on the kagome lattice, J. Phys. A: Math. Gen. **25**, 4335 (1992).

[71] A. Mielke and H. Tasaki, Ferromagnetism in the Hubbard model. examples from models with degenerate single-electron ground states, Commun. Math. Phys. **158**, 341 (1993).